Journal of Controlled Release 381 (2025) 113559

Contents lists available at ScienceDirect

Journal of Controlled Release

journal homepage: www.elsevier.com/locate/jconrel

Investigating the stability of RNA-lipid nanoparticles in biological fluids: Unveiling its crucial role for understanding LNP performance

Heyang Zhang [a,*], Matthias Barz [a,b,*]

[a] Division of BioTherapeutics, Leiden Academic Centre for Drug Research (LACDR), Leiden University, 2333CC Leiden, Netherlands
[b] Department of Dermatology, University Medical Center of the Johannes Gutenberg-University, 55128 Mainz, Germany

ARTICLE INFO

Keywords:
RNA-LNP
Physiological stability
Therapeutic efficacy
Analytical tool
PEG-free

ABSTRACT

Lipid nanoparticles (LNPs) are the most established and clinically advanced platform for RNA delivery. While significant efforts have been made to improve RNA delivery efficiency for improved protein production, the interplay between physiological stability, target specificity, and therapeutic efficacy of RNA-LNPs remains largely unexplored. This review highlights the crucial, yet often overlooked, impact of in vivo stability or instability of RNA-LNPs in contact with biological fluids on delivery performance. We discuss the various factors, including lipid composition, particle surface properties and interactions with proteins in physiological conditions, and provide an overview of the current methods for assessing RNA-LNP stability in biological fluids, such as dynamic laser light scattering, liquid chromatography, and fluorescent and radiolabeled techniques. In the final part, we propose strategies for enhancing stability, with a focus on shielding lipids. Therefore, this work highlights the importance of investigating and understanding the balance between stability and instability of LNPs in the biological context to achieve a more meaningful correlation between formulation properties and in vivo performance.

1. Introduction

Lipid nanoparticle (LNP) are the most established platform technology for in vivo RNA delivery, with four authorized RNA-LNP products targeting inherited and infection diseases. The rapid mixing of lipids and RNA allows for efficient access to LNP libraries differing in nanoparticle properties (e.g., size, surface charge, RNA payload content, packing density and internal structure), while ensuring encapsulation of RNA within the nanoparticle. The currently approved RNA-LNP drugs contain ionizable (cationic) lipid, helper lipid, cholesterol and PEG-lipid. Although the exact internal structure of RNA-LNPs is complex and non-uniform due to the lipid compositions and the complexity of the self-assembled particles, within these lipid structures RNA can be protected from hydrolysis/degradation. Moreover, depending on the composition, LNPs enable preferential RNA expression in specific organs (e.g., liver, spleen, lungs), enhance intracellular delivery and reduce RNA-associated immunogenicity.

Upon administration, LNPs interact with complex biological fluids, which differs in relation to the route. They either enter the bloodstream, get in touch with serum proteins and experience blood flow related shear forces or are taken up directly by cells at the injection site. For systemic application, however, the journey from the administration to the target site is fraught with challenges. Biological barriers, opsonization and degradation, along with the inherent susceptibility of RNA-LNPs to pre-release, aggregation and disassembly, can greatly impair therapeutic effects. Emerging evidence underlines that especially physiological stability of RNA-LNPs impacts their therapeutic efficacy, pharmacokinetics (PK), organ/tissue selectivity and toxicity. An extended circulation half-life seems crucial for RNA-LNPs to access extrahepatic tissues and/or accumulate in specific organs/tissues either by their inherent physicochemical properties (passive targeting), binding to plasma proteins (endogenous targeting) or specific ligands to interact with receptors on target cells (active targeting) [1]. For instance, around 90 % of the injected dose of mRNA-LNPs with Onpattro lipid compositions is cleared by the liver within half-an-hour following intravenous (i.v.) injection, limiting their therapeutic potential in non-hepatic diseases [2]. Although the therapeutic activity is achieved in this case, the stability of RNA-LNPs is of major importance for their biodistribution, required dose for positive therapeutic outcomes, and overall safety profile. Additionally, the limited stability of LNPs may be key to explain the commonly observed variations in biodistribution and therapeutic efficacy (protein expression or inhibition) across different

* Corresponding author at: Division of BioTherapeutics, Leiden Academic Centre for Drug Research (LACDR), Leiden University, 2333CC Leiden, Netherlands.
E-mail addresses: h.zhang@lacdr.leidenuniv.nl (H. Zhang), m.barz@lacdr.leidenuniv.nl (M. Barz).

https://doi.org/10.1016/j.jconrel.2025.02.055
Received 30 September 2024; Received in revised form 30 January 2025; Accepted 19 February 2025
Available online 27 February 2025

species, necessitating the optimization of lead candidates for each model. While composition of serum proteins remains comparable, the distribution volume and time to reach certain tissues differ largely between zebrafish, rodent, non-human primate and humans [3–6]. While this may affect to a lesser extent liver- or lung-targeted delivery (well accessible tissues), it constitutes a major issue for non-hepatic delivery (cancer cell uptake in solid tumors) and cell-specific uptake.

When exposed to biological fluids, biomacromolecules (e.g., serum proteins) spontaneously interact at the lipid-based nanoparticle surface through electrostatic, or hydrophobic interactions. This interaction leads to the formation of biomolecular corona on the LNP surface. The binding of specific serum proteins to the particle surface can also drive selective accumulation in different organs following i.v. injection [7]. In the case of LNPs, protein corona formation can also result in a dynamic exchange of lipid components with proteins (e.g., lipoproteins, lipid-bound albumin) in close proximity. These interactions impact the structural integrity, functional properties, PK, biodistribution and cellular uptake of LNPs, as demonstrated by Onpattro [8–10]. For example, plasma exposure can accelerate the desorption of lipid components more significantly than protein adsorption, highlighting the critical role of clotting factors in the degradation kinetics of mRNA-LNPs in plasma [11]. Overall, stability in a highly relevant and representative physiological context is a crucial factor to be taken into account when developing new formulations. Interestingly, researchers predominantly correlate LNP properties, such as size and ζ-potential measured in buffer, with in vivo protein expression/knock-down, or therapeutic response, while overlooking the interactions between particles and anatomical or physiological elements [12,13].

In this perspective, we provide an overview of RNA-LNPs, with a particular focus on their behavior in physiologically relevant environments, including factors governing stability, evaluation methods and strategies for improvement. In this review, physiological stability refers to the behavior of RNA-LNPs within biological conditions (e.g., serum, plasma), concerning their appearance (e.g., size, size distribution, morphology), structural integrity (e.g., disassembly, aggregation, circulation) and potency (e.g., bioactivity). Physical stability primarily concerns issues such as aggregation, fusion, and RNA leakage caused by various conditions (e.g., temperature, time, light exposure, buffer composition), and is typically assessed through direct (e.g., size, size distribution, morphology, RNA encapsulation) and indirect parameters (e.g., RNA integrity, bioactivity). For instance, aggregation (flocculation) and fusion (coalescence) are the most frequently reported modes of instability in RNA-LNPs [14,15]. Chemical instability arises from the susceptibility of lipids and RNA to various factors, such as oxidation, hydrolysis, enzymes, radiation and pH changes. For example, significant degradation was observed across all lipid components within 6 months, including SM-102 (9-Heptadecanyl 8-{(2-hydroxyethyl)[6-oxo-6-(undecyloxy)hexyl]amino}octanoate), DSPC (1,2-distearoyl-sn-glycero-3-phosphocholine), cholesterol and DMG-mPEG2k (1,2-dimyristoyl-rac-glycero-3-methoxypolyethylene glycol-2000), when mRNA-LNPs in liquid suspension was stored at 4 °C [16]. While no statistical alternations in size, polydispersity index (PDI), ζ-potential, RNA integrity or content were detected, a reduction in protein production was attributed to lipid oxidation induced by light exposure [17]. Also mRNA degradation in aqueous environments has been widely reported [18–20]. The physicochemical instability of RNA-LNPs not only undermines their stability and bioactivity but also raises safety concerns, and therefore ensuring long-term stability remains a significant challenge in the production and storage of RNA-LNP products, although various strategies (e.g., lyophilization, addition of stabilizer) have been explored [21–23]. Most importantly, we would like to highlight that the stability of RNA-LNPs can be analyzed in biological fluids by adopting established analytical methods, such as dynamic light scattering and fluorescence (cross)-correlation spectroscopy.

2. Factors influencing the physiological stability of RNA-LNPs

To date, certain factors have been identified that affect the physiological stability of RNA-LNPs. Given that RNA-LNPs are formed through a self-assembly process, during which the medium polarity increases rapidly, they are prone to yield structures in non-equilibrium states with inherent instability (Fig. 1). Therefore, maintaining the morphological and functional integrity of these assemblies within the dynamic and complex physiological environment is challenging and will require sophisticated optimization of LNPs. In addition, the inherent instability fosters cellular uptake, endosomal escape and cytosolic release of RNA. In this section, we aim to elucidate how each component/excipient impacts the stability of RNA-LNP formulations in physiological context. We will discuss the effects of modification (nature and quantity) to the lipids present in the shell (e.g., shielding lipid, helper and ionizable lipid) and core (e.g., ionizable lipid, sterol). Since the precise structural organization of RNA-LNPs and the detailed relationship between LNP structure and stability, however, is complex to analyze and thus remains poorly understood, we will focus less on structural details and more on the factors impacting stability. Nevertheless, understanding internal organization of lipid and non-lipid components within an LNP is another important area of research, but we would like to emphasize that correlating internal structures with in vivo stability and delivery efficacy together may be most meaningful for the directed development of LNPs.

2.1. Lipid composition

Shielding lipid. Shielding lipids, often with zwitterionic or neutral characteristics, primarily remain on and thus shape the surface of LNPs, providing electrostatic neutrality, steric repulsion and reduce unspecific interactions triggering recognition by cells of the immune system. Despite their minimal presence, these lipids play a critical role in LNP synthesis, maintaining storage stability, prolonging in vivo stability (circulation time) and maximize the therapeutic efficacy of RNA-LNPs under physiological conditions [24]. As Fig. 2A shows, polyethylene glycol (PEG)-conjugated lipids, such as DMG-PEG2k and methoxypolyethyleneglycoloxy(2000)-N,N-ditetradecylacetamide (ALC-0159), are commonly used to offer steric hindrance in aqueous solution and can reduce the protein corona formation, thereby improving the overall safety and efficacy of RNA-LNPs [25,26]. However, the hydrophilic shielding layer often fails to avoid protein absorption but reduces the interaction and fusion with plasma membrane. It is most likely that partial or full loss of the PEG-lipid coating might be beneficial to achieve more effective cellular uptake and endosomal translocation [27,28]. Taken together, the PEG shedding rate is crucial - if shedding too rapidly, LNPs may be primarily localized in the lungs, liver or immune cells in circulation or in the spleen, while shedding too slowly may hinder efficient cellular internalization and endosomal escape. There is considerable interest in fine-tuning the chemistry and density of PEG-lipids on LNPs surface, to achieve a reasonable balance between enhanced stability, extended circulation time and efficient intracellular delivery [29].

It is reported that PEGylation reduced protein binding in a ***PEG length***-dependent manner, with the sufficient inhibition of protein adsorption observed with PEG2k [28]. Unless otherwise stated, the PEG-lipid discussed here refers to linear PEG2k. Not only PEG chain length, the ***lipid anchor length*** also significantly impacts the PK and therapeutic activity of LNPs, since PEG-lipids are integrated into the LNP membrane through their hydrophobic tails. The impact conferred by PEG-lipids on LNPs' circulation time is determined by the dissociation rate of the PEG-lipid from the LNPs, which relates predominantly to the acyl chain length of the PEG-lipid. The longer dialkyl chains of PEG-lipid, the more energy is required for PEG-lipid to dissociate from the LNP and the higher the enthalpic barrier to dissolve in water as single molecule. The desorption rate was measured at 45 %/h (C14-PEG), 1.3 %/h (C16-PEG) and 0.2 %/h (C18-PEG) in siRNA-LNPs (MC3/DSPC/cholesterol/PEG-

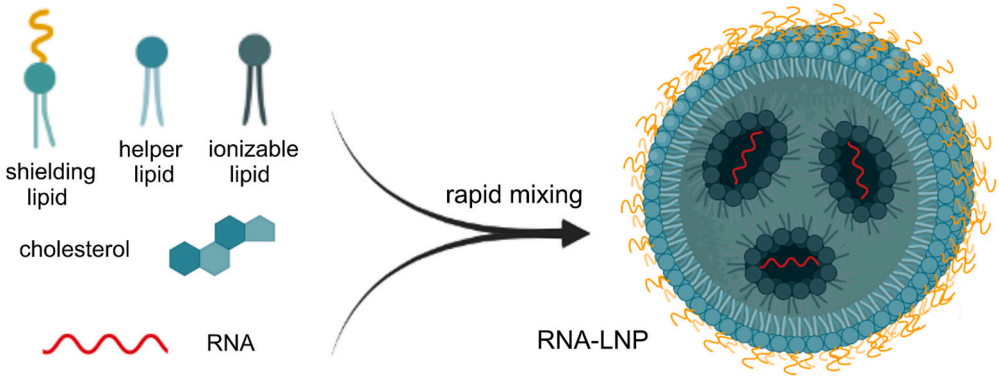

Fig. 1. Schematic representation of RNA-LNP synthesis.

lipid, molar ratio 50/10/38.5/1.5) by radiolabeling. Correspondingly, siRNA-LNPs exhibited slower clearance from the blood, with half-life of 0.9, 2.6 and 4.6 h respectively. This study, for the first time, comprehensively evaluated PEG-lipids in RNA-LNPs, considering both dialkyl chain length and PEG-lipid content, and identified 1.5 mol% of C14-PEG as the optimal amount of PEG-lipids that provides sufficient steric stabilization without considerably impacting hepatic gene silencing in vivo [30]. Likely, DSG-PEG-LNPs showed a longer circulation half-life in mice after i.v. injection compared to DMG-PEG-LNPs [31,32]. For siRNA-LNP (Onpattro), the shedding of DMG-PEG from LNPs during circulation allows the particles to interact with Apolipoprotein E (ApoE), and thereby promoting liver accumulation and the subsequent low-density lipoprotein receptor-mediated endocytosis into liver hepatocytes [9,30]. In addition, the shielding lipids on the particle surface reduces cellular internalization and endosomal escape because of steric hindrance, and a certain degree of structural fluidity or instability in LNPs can support intracellular RNA delivery. A very recent study showed that anti-PEG IgM was produced by LNP-associated PEG rather than free PEG. Compared to DMG-PEG, C16-PEG ceramide, which contains longer lipid tails, was less likely to shed from LNPs and consequently augmented anti-IgM production after repeated injection [33]. Besides, the use of polymer-lipid conjugates degrading into polymer and lipid tail upon extracellular triggers or during endocytosis is chemically possible but may require adaptation before use in LNPs due to the conditions of particle formation [34–36].

PEG conformation on the LNP surface is influenced by the surface PEG density, either a mushroom (sparsely packed) or more extended conformation (densely packed), depending on the proportion and architecture of PEG. It should be noted that the overall PEG density and the stretching of individual PEG chains is much lower than the one on polymer micelles or cylindrical bottlebrush polymers [37]. Increasing the ***proportion*** of PEG-lipid within LNPs extends their half-life, while a loss of surface PEG-lipid accelerates the dissociation of other lipids, likely due to the less lipid packing or structural defects. For instance, the dissociation of DSPC ($t_{1/2}$ 200 h vs 43 h) and MC3 ($t_{1/2}$ 19 h vs 12 h) from DSG-PEG-LNPs was significantly slower compared to DMG-PEG-LNPs in mouse plasma [31]. Increasing the total DSG-PEG in siRNA-LNPs from 2.5 mol% to 5 mol% resulted in a marked increase in circulation half-life from 30 min to over 8 h, and consequently enabled accumulation in distal tumors [38]. In comparison, the DMG-PEG content in mRNA-LNPs didn't affect hEPO production following the first and second i.v. administration [33]. In addition to the surface density, increasing the PEG-lipid content led to smaller RNA-LNPs ranging from 120 nm (0.25 mol%) to 25 nm (5 mol%), with siRNA-LNP stability being size-dependent, as determined by dynamic light scattering using the Malvern Zetasizer NanoZS [31,39]. The architecture and terminal group of PEG are another noteworthy determinants of the performance and shielding efficacy of PEG-LNPs [40]. Taken together, the shielding effect is related to the proportion of PEG-lipid as well as the structure and length of the PEG chain and lipid tail. This is also true for other shielding lipopolymers (e.g., polysarcosine-lipids) [41].

The pivotal role of PEG-lipids in RNA-LNPs quality has been well demonstrated in clinical applications. Alongside with the benefits, unexpected immune reactions such as accelerated blood clearance and hypersensitivity reactions, have been raised as major concerns for PEG-LNPs [40]. Efforts to eliminate or reduce the undesirable immune responses and improve the safety and efficacy of PEGylated RNA-LNPs will be discussed in **Section 4**.

Ionizable lipid. Ionizable amino lipid plays active roles in assembly process and the final properties of RNA-LNPs. Ionizable lipid generally consists of a hydrophilic headgroup (e.g., chemistry, number of ionizable head), a linker and hydrocarbon tail (e.g., number, length, saturation, branching of the tails) (Fig. 2B). As a gold standard for RNA-LNP formulations, MC3 features two C18 fatty acid (aliphatic) ***tails*** and is not fully degradable in vivo, resulting in a long tissue half-life [42,43]. To enhance biocompatibility, PK, potency and safety, ionizable amino lipids have been explored, which contain degradable chemical moieties (e.g., ester, amide, mercaptan) linking ionizable group and aliphatic tail [44]. The introduction of degradable groups has already demonstrated a substantial enhancement of biocompatibility of cationic lipids, while their activity is largely maintained [45,46]. Due to its simple structure, good chemical stability and ability to undergo hydrolytic degradation, an ester linkage was introduced into the hydrophobic alkyl chains of MC3. By replacing the 9,10-*cis* double bond with an ester functionality centrally within the hydrocarbon chain (LC319), siRNA-LNPs exhibited a rapid plasma elimination ($t_{1/2} < 30$ min) and tissue clearance. In contrast, L343, which contains a metabolically more stable, sterically hindered tert-butyl ester, exhibited slower plasma elimination and higher, more persistent levels in the liver [47]. The potency of ester-containing amino lipid has also been explored in mRNA-LNPs. By replacing the lipid tail of MC3 with a primary ester lipid tail, Lipid 5 showed a faster plasma clearance ($t_{1/2}$ 1.2 h vs 8.4 h), improved endosomal escape efficiency (15 % vs 2.5 %) that likely caused by faster desorption rates after degradation and more fusogenic lipid tail, and increased protein production in non-human primates [43]. In another study, substituting the amide linker in βN2 with an ester linker between an amine core and hydrocarbon tails resulted in a significantly shorter half-life in mouse plasma ($t_{1/2}$ 15 h vs 295 h) following i.v. injection of mRNA-LNPs [48]. Additionally, the distance between the anime headgroup and the linker in DLin-K-DMA was found to affect the dissociation constant from siRNA-LNPs [49].

Several innovative modifications to the headgroup, lipid tail and content have shown improved RNA delivery efficiency in vivo through various mechanisms (e.g., enhancing endosomal escape, improving mRNA affinity). However, the relationship between these modifications and key properties, such as physiological stability and therapeutic efficacy, of RNA-LNPs remains insufficiently explored [50–54].

Helper lipid. Helper lipids are typically zwitterionic lipids with

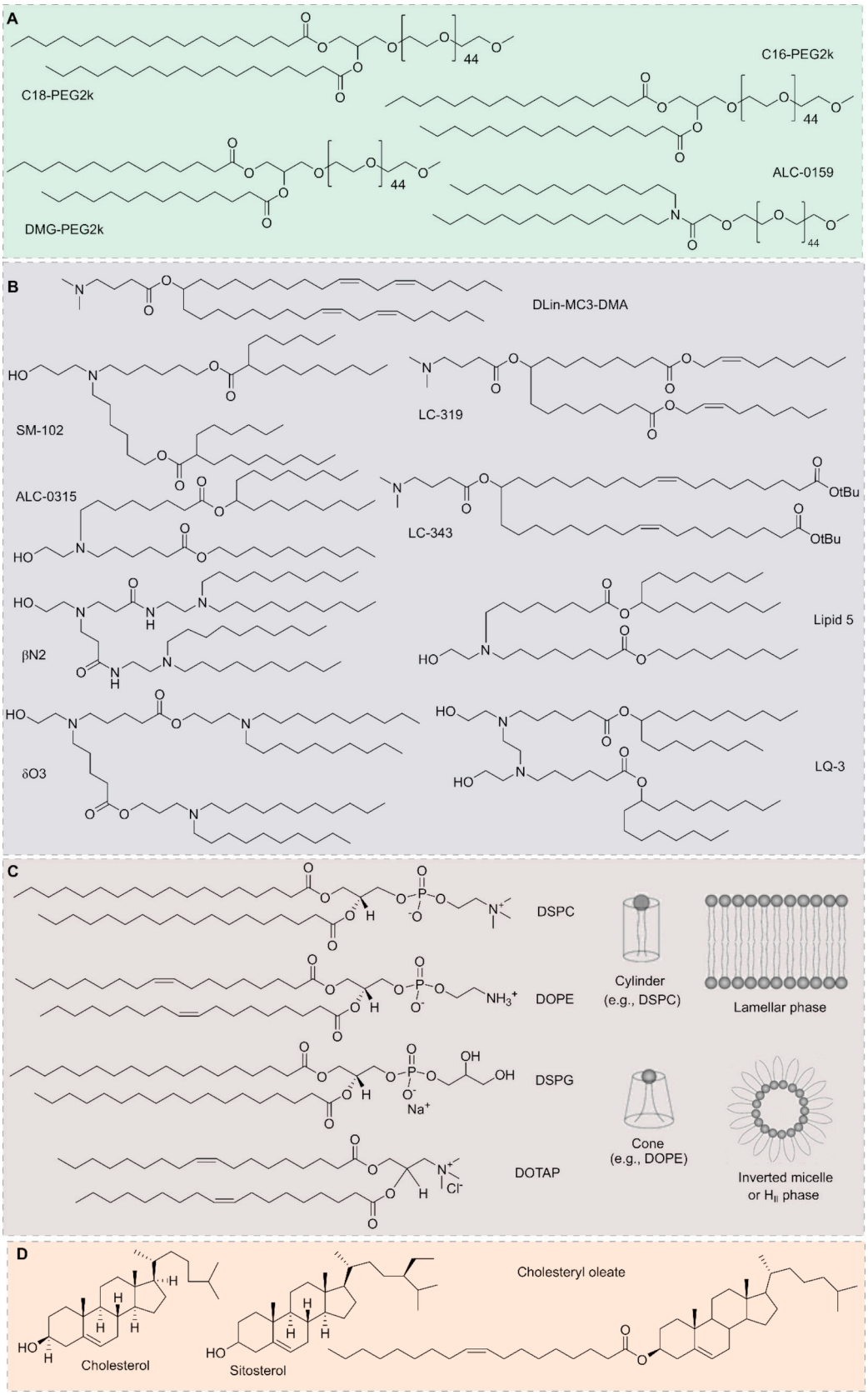

Fig. 2. Chemical structure of important LNP components.

varying alkyl chain saturations, chain lengths, and polar head group substitutions, such as DSPC, DOPC and DOPE, assist in the formation, and substantially contribute to the overall stability of RNA-LNPs (Fig. 2C). Among these, DOPE and DSPC are the two of most extensively used helper phospholipids for LNP formulation in both preclinical and clinical studies. DSPC, characterized by its cylindrical molecular geometry, strongly favors bilayer formation; while DOPE, with its cone-shaped molecular geometry, tends to form non-lamellar structures, such as hexagonal phase (H_{II}) [55]. This is reflected by the morphology of mRNA-LNPs, where liposome-like protrusions or irregular surface structures were more likely found in DSPC-LNPs. Note that replacing DSPC with DOPE resulted in the loss of bleb-like structures, which was not always true, as we also found blebbed structures in DOPE-containing mRNA-LNPs, which is likely due to the slower ethanol dilution within manual mixing, and thus more heterogeneous particle formation [14,56]. In turn, such blebbed structures are not always present in RNA-LNPs; for example, siRNA-LNPs exhibit an electron-dense core structure regardless of the helper lipid (DSPC or DOPE) [57]. Functionally, DOPE destabilizes the endosomal membrane by transitioning from lamellar to H_{II} phase under acidic conditions, facilitates endosomal escape and provokes more efficient RNA release and thus more robust cytosolic RNA delivery [58,59]. It is noteworthy that the direct interactions of the ionizable cationic lipid alone may not fully capture the extent of RNA packing and protection; rather, these interactions occur synergistically with the helper lipid. For instance, as shown by molecular dynamics stimulations, the difference in RNA binding affinity between DLinDAP and DLinDMA was minimal, but was greatly enhanced in the presence of helper phospholipid (DSPC or DOPE). DLinDAP tends to form stronger direct interactions with RNA and envelop RNA to a larger extent than DLinDMA-based formulations. This is likely due to a higher degree of swelling and therefore a larger total surface area of RNA in contact with DLinDAP. In addition, larger RNA binding affinities for both phospholipids and cholesterol was reported in the presence of DOPE compared to DSPC. On the other hand, the impact of the same helper phospholipid on LNP performance depends on the formulations in which it appears, more specifically on the ionizable lipid. Replacing DSPC with DOPE induced a reduction in the median distance of RNA to the bilayer in DLinDMA formulations, which was not observed in DLinDAP formulations [60]. For example, a decrease in DSPC content in LQ-3-LNPs has shown an elevated mRNA delivery efficacy, achieving maximal efficacy in the absence of DSPC, whereas reduced DSPC content resulted in increased PDI and decreased mRNA transfection efficiency in SM-102 formulations [61]. This is likely ascribed to the stronger interaction affinity for LQ-3 lipid with mRNA compared to SM-102. Thus, the choice and content of helper lipids must be carefully optimized for each specific LNP formulation to ensure the desired RNA therapeutic performance, as well as to meet production requirements. In the context of RNA-LNPs, DOPE exhibits stronger interactions with other lipids or physiological context. Molecular dynamics simulations have shown that DOPE strongly interacts with the lipid tails and carbonyl oxygens of MC3, which was not observed with DSPC [62]. DOPE-LNPs also exhibit stronger interactions with ApoE than DSPC-LNPs, and preferentially accumulate in the liver whereas DSPC-LNPs tend to accumulate in the spleen [63]. Despite extensive research, a reliable head-to-head comparison of the physiological stability between DSPC-LNPs and DOPE-LNPs has not yet been reported. Recently, Chander et al. found that with 10 mol% DSPC, MC3-containing mRNA-LNPs degraded at a rate of 20 %/h in 50 % FBS, with a circulation half-life of 0.26 h. Replacing 10 mol% DSPC with 40 mol% egg sphingomyelin considerably declined the degradation rate to 5 %/h, and extended the circulation half-life to 3.66 h. This improvement is likely due to the higher helper lipid content fostering the presence of exterior lipid bilayer [2].

Substituting DOPE with charged alternatives (e.g., DOPS, DOTAP) in LNPs was found to improve mRNA delivery to the spleen and lungs. For DOPS-containing LNPs, a shift to spleen was mediated via the PS-specific receptor Tim4 that presents on the marginal zone macrophages of the spleen. In addition to the role of protein corona on the surface of cationic LNPs, other potential mechanisms could be responsible for the lung specificity, such as the electrostatic interaction with heparan sulfate proteoglycans in the glycocalyx around the alveolar endothelial cells and proteoglycans, as well as the more susceptibility of lung cells to the membrane destabilization caused by cationic lipids [12]. Such shift in the organ specificity has been reported in selective organ targeting (SORT) LNPs, in which a charged helper lipid and DOPE were added to regulate the organ specificity [13].

Cholesterol. Cholesterol, a natural component of cell membrane, is crucial for structural stability of LNPs, since they govern lipid packing, membrane fluidity and permeability as well as physiological stability (circulation in bloodstream) of RNA-LNPs, although its precise localization within RNA-LNPs remains ambiguous (Fig. 2D). Decreasing cholesterol ***content*** in mRNA-LNPs (SS-OP (or MC3)/DOPC/cholesterol/DMG-PEG2k) caused more degradation in systemic circulating blood and reduced expression level in the liver [64]. Conversely, increasing the proportion of cholesterol in the PEGylated siRNA-LNPs from 30 to 50 mol% improved LNPs stability in blood circulation in terms of siRNA leakage and silencing activity in mice [65]. The chemical structure of cholesterol not only affects RNA-LNPs structure but also distribution and delivery efficacy. For example, modifications to the cholesterol backbone, such as the addition of methyl and ethyl groups to the C24 alkyl tail, have been shown to induce multilamellarity (>50 % increase compared to cholesterol). In contrast, introducing a double bond led to lipid partitioning, with over 90 % increase compared to cholesterol [66]. β-sitosterol-LNPs caused an evolution (a rearrangement/fusion of LNP) towards larger particles in bovine serum, compared to the cholesterol-LNPs [67]. As Paunovska et al. reported, LNPs formulated with cholesteryl oleate led to more efficient and selective RNA (siRNA or sgRNA) delivery to hepatic endothelial cells in mice, than the LNPs analogues containing unmodified cholesterol. Notably, this study also found a higher delivery efficiency to hepatocytes than to liver endothelial cells, suggesting oleate cholesterol-LNPs more potential in hepatocyte-targeted delivery [68]. Since structural modifications of cholesterol in vivo can result from oxidation or interactions with lipoproteins during trafficking, they further studied the oxidized cholesterol in mRNA delivery. LNPs containing oxidized cholesterol preferentially delivered mRNA to cells within the liver microenvironment (Kuffer cells, liver endothelial cells) than to hepatocytes. And oxidation on the hydrocarbon tail attached to sterol ring D exhibited greater tolerance than the LNPs containing cholesterol modified on sterol ring B. This may be attributed to differences in overall stability or differences in interactions with serum proteins, which in turn affects cellular targeting and delivery efficiency [69–71]. Due to the multifaceted role in LNPs and dynamic behavior in vivo, the relationship between cholesterol structure and LNPs' stability in biological contexts remains largely underexplored.

Taken together, RNA-LNPs are self-assembled structures comprising various lipid components, cholesterol, and RNA molecules. In addition to the individual lipid chemistry, the overall amount (relative to RNA) and the ratio of lipid components within the LNP formulation contributes to the overall properties. That said, increasing the content of one component often necessitates the changes at expense of another lipid component, leading to a complex interplay that affects the overall stability, functionality, and ex vivo or in vivo behavior of RNA-LNPs. It is indeed a detailed understanding of the internal order of lipids within the LNP is not only scientifically interesting but also of major importance to understand molecular reason for stability and nucleic acid protection and release. Determining the internal structure on molecular level, however, will be a complex endeavor and will require single particle analysis of large number of particles per individual formulation due to the inhomogeneity of LNPs. The currently applied ensemble methods such as small angle X-scattering will provide only limited molecular information [14,72]. Therefore, we believe such studies may be worth all efforts, if it is clear that the LNPs to be analyzed do not change organization immediately when in contact with serum proteins or other

components of biological fluids. Moreover, previous studies reveal that it is major challenge to predict mRNA-LNP efficacy based on RNAi efficiency and vice versa due to the differences in structure, size, net charge, stability, and mode of action between different nucleic acid types [44,56]. Therefore, the final properties and performance of RNA-LNPs depend on this intricate balance of lipid composition and nucleic acid payload.

2.2. Surface properties

Extracellular interactions, influenced by surface composition and the presence of extracellular proteins at the administration site, determine the fate of RNA-LNPs. The surface properties, including surface charge and the presence of functional groups (e.g., PEG, ligand), play a pivotal role in how LNPs interact with their biological environments.

Surface charge is an important indicator and influencing factor of LNPs stability, and stable, well-dispersed particles maintain longer circulation [73]. RNA-LNPs with neutral or slightly negative surface are favorable to reduce nonspecific binding to plasma proteins and minimize interactions with immune cells, leading to prolonged circulation, while they may tend to aggregate over time owing to the limited interparticle repulsion [44]. While charges can be used to stabilize colloidal systems in buffer by repulsive electrostatic interactions, the highly cationic or anionic LNPs tend to attract oppositely charged blood components by electrostatic and entropy driven interactions (salt pair release), increasing their recognition and clearance by the mononuclear phagocytic system [8,74]. Most mRNA-LNPs (-5 mV) display extended circulating in zebrafish embryo, while anionic mRNA-LNPs (-22 mV), generated by substituting DSPC with DSPG, were predominantly redirected within sinusoidal endothelial cells via scavenger receptors [75]. This underlines the fact that the formation of a protein corona is predominantly driven by entropic factors (salt-pair release) and to a much lesser extend by enthalpic factors (ionic interactions) [8]. The surface charge can be tuned by PEG density. For example, the surface charge of siRNA-LNPs at pH 5.5 dropped from +32 mV to +18 mV when PEG-lipid content increased from 1.5 mol% to 10 mol%, indicating that increasing PEG density shields surface charge of LNPs [25]. A denser PEG layer on the surface of mRNA-LNPs seems more favorable for stealthy effect of nanocarriers but lowers interactions with cells [76]. As well, substituting neutral helper lipid DOPE with anionic or cationic lipid, or altering their content resulted in the changes in surface charge, and consequently led to a pronounced and consistent specificity shift of mRNA-LNP in vivo to the spleen (anionic) or lungs (cationic) as comment above, which may -especially in the case of lungs- relate to pronounced aggregation events [12]. By coupling the negatively charged (Glu-urea-Lys) targeting ligand to DSG-PEG, siRNA-LNPs exhibited comparable circulation properties ($t_{1/2}$ 10-12 h) to the plain LNPs, but reduced cellular uptake [38].

Up to now, there has not been a publication reporting the absence of protein corona formation on LNPs when exposed to biofluids, while on core-crosslinked micelles and cylindrical bottlebrush polymers, protein adsorption can be blocked entirely [77]. Additionally, quantitative reports on LNP stability in biological fluids are lacking, while methods for the determination of protein in close proximity to the surface of lipid-based nanoparticles have emerged [78]. From our point the most interesting question is do we really see the formation of a protein corona on LNPs or does the formation of more complex LNP/protein aggregates occurs. In any case, the interaction with proteins has a crucial influence on stability, circulation time, and biodistribution of LNPs. PEGylation as discussed above, can enhance the stability and circulation time of LNPs by providing a steric barrier against protein adsorption and immune recognition, but the introduction of a dense PEG layer on the surface of LNPs requires high PEG densities leading to a transition of polymers in mushroom conformation (PEG in a more random coil state) to an extended state (stretched main chain conformation). Since the stretching of polymers requires energy and is accompanied by a loss of conformational entropy, stretching on PEG chains of PEGylated lipids on LNPs will be limited even at higher content of such lipids. Beyond surface charge alternations and steric shielding, modifying the surface of LNPs with chemical moieties (e.g., dye, ligand, antibody) influences properties further and may compromise stability in physiological fluids. For instance, mannose-DSPE-PEG coating on siRNA-LNPs didn't induce any significant difference in surface charge, morphology and size, yet it successfully achieved efficient spleen accumulation, indicating specific interactions with mannose receptors on immune cells in the spleen [79].

Other physicochemical properties influenced by surface modification, for instance, size, shape and internal order are important parameters influencing the stability, tissue penetration, PK, biodistribution and therapeutic efficacy of RNA-LNPs. Small LNPs (<30 nm) are generally preferrable for enhanced tissue or tumor penetration, but they often exhibit limited nucleic acid content, shielding and stability in serum or plasma [65]. For example, siRNA-LNPs (45 nm) exhibited a significantly faster lipid dissociation rate in mouse plasma compared to larger LNPs (80 nm), with the half-lives of MC3 ($t_{1/2}$ 4.9 vs 12 h), DMG-PEG2k (1.1 vs 1.7 h), and DSPC (6.2 vs 43 h), respectively [31]. In addition, the smaller LNPs (around 100 nm) seemed to be less immunogenic in mice compared to the larger counterparts with respect to IgG antibody titers [80]. In contrast, Chen et al. reported that larger LNPs might be unable to penetrate the 100-140 nm fenestrations in liver vasculature, therefore limiting LNP biodistribution in the liver [31]. Thus, careful consideration of surface charge, coating materials, and functionalization is essential to optimize LNP design for effective and sustained RNA delivery.

2.3. Internal structure

Internal structure of RNA-LNPs are also critical to governing LNP stability in buffer and under physiological conditions. Since RNA-LNP synthesis involves rapid mixing of multiple components at room temperature as well as different solvents, the resulting LNPs may not necessarily reach a thermodynamic equilibrated state as discussed above. Small changes in composition (e.g., lipid, RNA, buffer composition), synthesis methods, storage conditions or pre-analysis handling can lead to great structural changes [81]. For instance, Cheng et al. reported a difference in the bleb fraction (59 % in sodium citrate buffer vs 5 % in sodium acetate buffer, both at 300 mM) using the same lipid composition [82]. More importantly, RNA cargo plays a key role in LNPs assembly. For small RNA, such as siRNA, their small size, double stranded character and higher diffusivity, facilitate better mixing with the ionizable lipids, leading to more uniform structural arrangement (e.g., multilamellar structures where siRNA molecules are sandwiched between bilayer lipid assemblies) and fewer empty LNPs, although bleb-shaped structures on the surface of siRNA-LNPs were also reported [57,83]. In contrast, large RNA molecules, such as mRNA, adopt complex secondary and tertiary structures driven primarily by base stacking, hydrogen bonding and electrostatic stabilization, thus resulting less uniform LNPs [84]. For example, bleb structures were observed in 20 % DSPC-LNPs encapsulating mRNA and DOPE-LNPs, while the precise internal structure of mRNA-LNPs has not yet been clearly identified through direct experimental methods [14,56]. Other external factors may contribute to the formation of blebs, such as freezing [85,86]. Thus, the common representations as a sphere with RNA lipid-bound in the core, may not fully capture the complexity of mRNA-LNP structures. Instead, mRNA-LNPs might be more accurately represented as a continuum of structural states corresponding to varying mRNA-lipid association degrees. Nevertheless, it is challenging to conclude on the precise role of a certain internal structure in the stability of RNA-LNPs, since we lack knowledge and understanding on the molecular internal structure of LNPS related to a certain lipid and nucleic acid composition. Several other key questions remain unknown, such as the kinetics of blebs formation, the types of blebs and the extend of blebbing (e.g., multiple blebs per LNP and proportion of bleb-containing LNPs), whether these structures are maintained in biological environments, and their

potential correlation with physiological stability, cell specificity and transfection efficacy [81].

2.4. Administration route

The biodistribution, PK and therapeutic outcomes of RNA-LNP formulations are greatly influenced by the administration route (e.g., i.v., intramuscular (i.m.), subcutaneous (s.c.), intradermal (i.d.). intraperitoneal (i.p.)). The two approved mRNA-LNP vaccines for Covid-19 are administered intramuscularly to elicit robust immune response, by either local transfection of antigen-presenting cells (APCs) in the muscle, which then migrate to the lymphatics, or by passive drainage through the lymphatic system, delivering mRNA directly to APCs and T cells residing in nearby lymph nodes [87]. As determined by LC/MS, almost 15 % of the injected dose of deuterium-labeled cholesterol contained in mRNA-LNPs was detected in the blood 2 h after i.m. injection, but stability of the LNP itself remains unclear. For (DiR-labeled) luciferase-encoding mRNA LNPs (< 200 nm) administered intramuscularly, lymphatic drainage is the primary route for rapid entering into the systemic circulation, rather than being constrained in the muscle tissue. Larger mRNA-LNPs mostly remain at the injection site while smaller LNPs are more likely to migrate to the liver, as visualized using IVIS imaging. Since the DiR molecules incorporated in LNPs likely leaked over time, in situ hybridization using Cy5-labeled mRNA sequence probes was employed to visualize the only released mRNA in the liver, muscle and lymph node, demonstrating the most robust transient gene delivery in the lymph nodes. Intravenously injected LNPs accumulated mainly in the liver and produced proteins as early as 1 h after injection, while there was a delay in protein expression at the injection site after intramuscular injection. Subcutaneously injected LNPs tend to remain localized at the injection site, resulting in localized and much weaker protein expression [88]. LNPs administered intraperitoneally are less likely to enter the bloodstream directly from the peritoneal cavity, instead draining into the lymphatic system via diaphragmatic lymphatics [89]. Hajj et al. compared the distribution and protein expression of mRNA-LNPs following i.v., s.c., i.m., and i.p. injection. Both distribution and protein production primarily were observed in the liver through i.v. and i.p. injection, while i.m. and s.c., yielded protein expression at the injection site [90].

Each administration route presents unique biological barriers, necessitating tailored LNP formulations optimized for the specific research or therapeutic goals [91,92]. Inhalation, for example, is emerging more and more as a promising approach for the delivery of mRNA to the lungs. The lungs offer a large surface area for absorption; while the respiratory tract is highly heterogeneous and consists of the upper conducting zone, which contains mucus-secreting epithelial cells, and the lower respiratory zone with a thinner epithelium cell layer [93]. The therapeutic efficacy of RNA-LNPs in this context is highly dependent on their stability, since during nebulization or spraying, significant mechanical stress from shear forces and air-water interface can compromise their structural integrity and morphology. Moreover, LNPs trapped in the luminal mucus layer as individual nanoparticle or aggregates are transported upwards and eventually eliminated through coughing or swallowing over time. PEGylation is a widely used approach to provide steric hindrance that prevents aggregation and to facilitate penetration through this mucus layer [94,95]. For example, Kim et al. observed mRNA leakage during nebulization because of the structural rearrangement of LNPs, and a higher content of DMG-PEG2k helped retain the encapsulated mRNA. However, a PEG-related trade-off between particle stability and protein production in the lungs of mice was reported [96]. Ongun et al. found that increasing the PEG-lipid content enhanced colloidal stability during aerosolization, maintaining particle size and morphology. Yet, this increase in PEG-lipid content was associated with reduced transfection efficiency [97]. Overall, LNP formulations with low PEG-lipid content (1-5 mol%) tend to offer a favorable balance between colloidal stability and transfection efficiency, though further optimization is needed to maximize protein expression in vivo [93,98].

Different tissues differ in the type of proteins at the injection site. For example, exposure to serum albumin or full serum induced changes in both size and morphology of LNPs, which cannot be observed in the presence of fibrinogen [99]. Once binding to ApoE, a redistribution of lipids can occur both at shell and core of mRNA-LNP, leading to a rearrangement of internal structure of particles and mRNA release [100,101]. Moreover, individual physiological states, such as obesity, can impact the LNP function through corona formation. LNP coronas derived from obese plasma contained 1.8-fold more protein than those derived from lean plasma, while the ApoE abundance was moderately reduced. In obese plasma, there was notable increase in the binding of lipid-associated, amphipathic and apolipoproteins to the LNPs [10].

3. Methods/techniques available to test biological stability

To understand the pivotal role of proteins on LNPs, monitoring these interactions in diverse biological settings is in high demand but remains challenging due to the lack of reliable and robust analytical techniques under representative physiological conditions. Discriminating between formation of a protein corona (preservation of LNPs structure) or formation of aggregates (massive rearrangement of LNP structure) seems pivotal in understanding the correlation of a certain LNP composition and biodistribution or mRNA expression (Fig. 3). For instance, conventional single angle dynamic laser light scattering is commonly used to measure the size of LNPs, but it is -besides it's general inaccuracy- not directly applicable to measurements in biological fluids even when the serum is diluted to 10 % or less. Since serum proteins were found in a trimodal size distribution with typical mean radii (approximately 3–5 nm, 17–30 nm, 70–150 nm), particle sizes between 10 and 100 nm or changes of these values cannot be characterized properly even in diluted serum [102–104]. In addition, diluted serum does not replicate the physiological environment of the bloodstream, where factors such as protein concentration and flow dynamics differ significantly. As discussed, the PEG-lipid shedding rate decreases with serum dilution, suggesting that in vivo conditions, where dilution is more severe upon intravenous injection, may result in a much faster shedding rate. Currently, there is no quantitative correlation between PEG-shedding rates observed in non-diluted serum or plasma and the plasma clearance of LNPs in vivo [105]. This highlights the need for more sophisticated analytical tools to better understand and predict the behavior of LNPs in the body. Several techniques are indeed established and applicable to the analysis of LNPs in biological fluids without the need for dilution (Fig. 4).

3.1. Light scattering

Physicochemical properties, such as size, PDI and ζ-potential, are the widely used indicators of colloidal stability of LNPs. Size and PDI are among the most frequently monitored parameters, and are typically characterized using ensemble methods, such as dynamic light scattering and nanoparticle tracking analysis. Dynamic light scattering (DLS) is a most commonly used tool to determine the size (hydrodynamic diameter, D_h) and distribution of particles, by measuring the fluctuations in light scattering caused by particles undergoing Brownian motion in the observation volume which provides access to the average diffusion coefficient of nanoparticles [106]. Commercial DLS instruments, operating at a fixed detection angle (e.g., 173°), have several limitations. The correlation function at a single scattering angle, does not allow for structural or morphology-related information [102]. Moreover, the obtained data describes size and dispersity only in the case of monodisperse, spherical, small nanoparticles (well below 100 nm). For larger nanoparticles, a strong angle dependency of the diffusion coefficient (derived from the corresponding autocorrelation function) can occur requiring measurements at multiple angles and extrapolation of the q

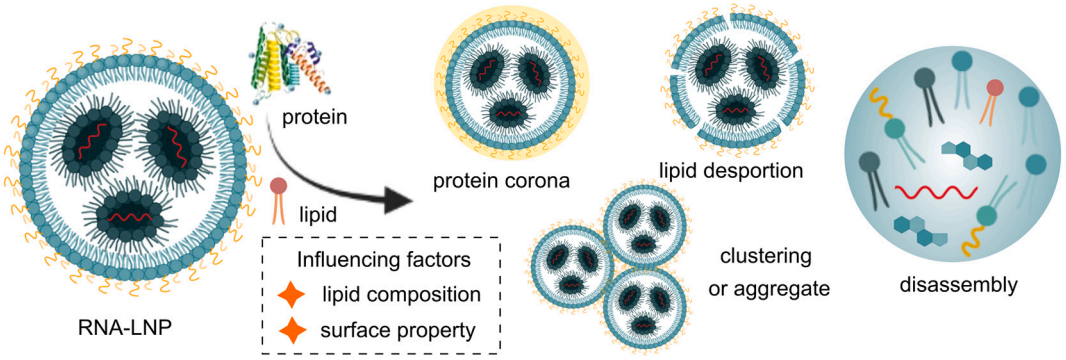

Fig. 3. Instability of RNA-LNPs in physiological environment and the influencing factors. Interactions with proteins or endogenous lipids can lead to the formation of a protein corona, clustering or aggregation, lipid component desorption, and, in some cases, the complete disassembly of the LNPs.

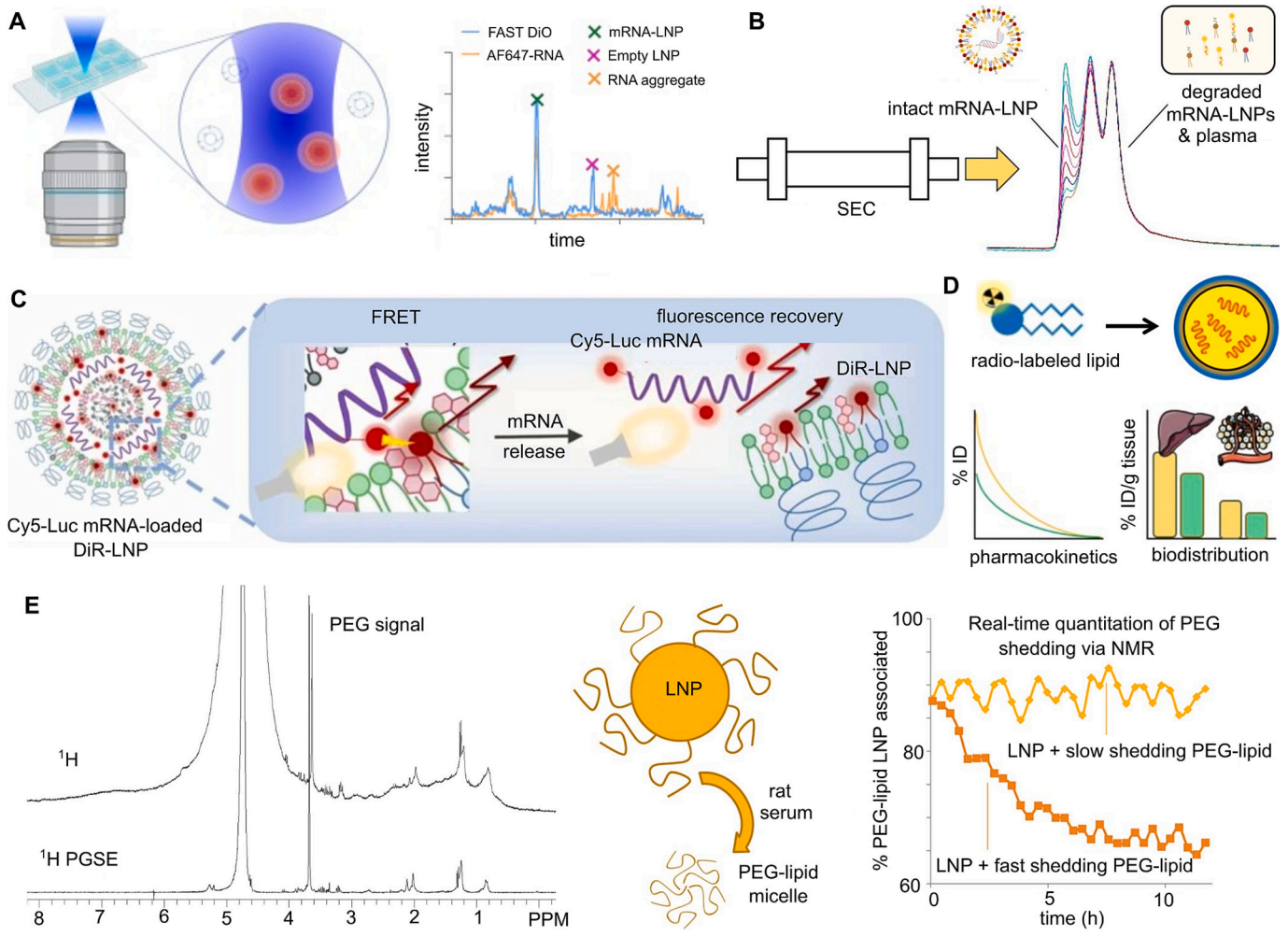

Fig. 4. Representative scheme of methods that are currently available to assess the stability of RNA-LNPs in physiological context, including (A) Fluorescence Correlation Spectroscopy (FCS), (B) Size-exclusion chromatography (SEC), (C) Förster Resonance Energy Transfer (FRET), (D) radioactive labeling and (E) Nuclear Magnetic Resonance (NMR). Reproduced with permission from Ref [11, 105, 119, 134, 137].

vector to 0. Under these conditions single angle measurements are not able to determine the proper average size and PDI [107]. As mentioned above, human serum/plasma constitutes of proteins of three different size regiments. Therefore, the contribution of such particles needs to be considered. Manfred Schmidt and coworkers developed a methodology to analyze nanoparticles in full serum by DLS already in 2010 [104]. Usually, a biexponential fit is applied to the correlation function of LNPs to consider their polydispersity. The fit of the serum correlation function is more complex and requires a sum of three exponentials (for each of the three size regiments). Now LNPs are added to the serum/plasma and analyzed by DLS. While for LNPs above 200 nm the size increases can be studied directly, for smaller particles only the effect of the LNP on the aggregation state of serum proteins can be investigated. If no aggregation occurs, the correlation function of the particles in serum solution, can be perfectly fitted by the sum of the individual correlation functions. In case of serum induced LNP aggregation, one cannot satisfactorily fit

the correlation function as sum individual correlation functions of the particle/serum mixture anymore, but an additional exponential fit function is required for the aggregates being formed. Since DLS is highly sensitive to larger particles, the described methodology allows -at least- to ensure the absence of LNP induced formation of larger aggregates. Since the scattering contribution of large aggregates is much larger at smaller angels than larger angles (e.g., 90° or 173°), DLS with detection at multi-angles (MADLS) is required to perform the described analysis properly [108,109]. In our previous work, MADLS analysis revealed a slight angle dependency for mRNA-LNPs, which may be attributed to their moderate dispersity and size [14].

3.2. Fluorescence correlation spectroscopy (FCS)

Besides using fluctuations in the intensity from scattered light, nanoparticles can also be characterized by measuring the diffusion coefficient by correlating fluctuation in fluorescence intensity. In Fluorescence Correlation Spectroscopy (FCS) the diffusion of fluorescent molecules or particles in and out of a small-excitation focal volume (fluorescence intensity fluctuations) is subjected to an auto-correlation analysis, which provides information on the concentration, diffusion coefficient, and brightness of fluorescent molecules or particles (Fig. 4A) [92,110,111]. The stability of fluorescent RNA-LNPs, containing either fluorescently labeled RNA cargo, lipophilic dyes or fluorescent lipid components, therefore, can be monitored through brightness, where an increase in brightness indicates potential aggregation, or by the diffusion coefficient, where a decrease indicates the presence of larger particles [112,113]. Furthermore, dual-labeled particles can be examined using Fluorescence Cross-Correlation Spectroscopy (FCCS). When fluorescent particles diffuse through the diffraction-limited observation volume, fluorescence fluctuations from multiple channels are recorded. Individual peaks are analyzed with respect to the brightness, width, and co-occurrence with another color. Like FCS, peak brightness can indicate particle clustering, and combined with peak width analysis, it can detect large particles or aggregates. Cross-correlation of peaks in multiple channels enables localization and quantification of RNA cargo, especially in RNA-LNPs containing both fluorescent RNA and LNP. By combining multiphoton excitation with FCS, Fu et al. demonstrated that in vivo FCS can dynamically track fluorescent nanoparticles (e.g., dextran, Quantum dots and polymer dots) in the brain of a live mouse with excellent spatial and temporal resolution, enabling measurement of nanoparticle half-life. Importantly, they also observed the dissociation of fluorophores from particles, allowing for the monitoring of nanoparticle degradation [114]. FCCS can also be combined with techniques, like FRET, to explore assembly stability, particularly those containing small nucleic acids (e.g., siRNA, antisense oligonucleotides), such as lipoplexes and polyplexes [115–118]. Recently, Sych et al. reported an assay, single-particle profiling (SPP), for studying the content and biophysical profiling of mRNA-LNPs smaller than 200 nm. Unlike FCCS, which reduces all fluctuations into a single curve, SPP identifies individual peaks in intensity fluctuations in multiple channels, enabling detection of clustering, large particles or aggregates, and quantification of RNA payload. It is worth noting that F(*C*)CS and SPP, are able to directly visualize and quantify encapsulation by measuring the co-occurrence of mRNA and lipid dye signals for each particle, revealing loading capacity and encapsulation heterogeneity. This distinguishes from the bulk methods such as the RiboGreen assay, which only gives an overall percentage of loading efficiency without any insight into the cargo distribution [119].

3.3. Nanoparticle tracking analysis (NTA)

Nanoparticle Tracking Analysis (NTA) tracks the movement of (fluorescent) particles under Brownian motion in an observation volume to determine the individual diffusion coefficients, which can be used to determine R_h [120]. Unlike DLS, NTA tracks individual particle movements to calculate the diffusion coefficient for each individual particle, thus allowing for an analysis of differences between two particles or populations, without bias towards larger particles or aggregates [121]. In addition to particle concentration measurements, NTA is a single particle analysis method but able to determine size distribution profiles when the data of individual particles is compiled. In addition, the analysis can be performed in complex media (e.g., blood plasma, serum, cell culture media). For example, for C14-PEG-LNPs, there was an increased size and decreased particle concentration over time in FBS, indicating the protein absorption around particles [122]. Liu et al. visualized and quantified the particle concentration and size distribution of mRNA-LNPs, coronated LNPs, and endogenous nano-sized particles in blood plasmas using NTA [10].

3.4. Liquid chromatography

Size-exclusion chromatograph (SEC) is a widely recognized technique for size-based separation. In SEC, particles are separated based on their size, as they pass through a column packed with a stationary phase containing porous materials. Larger particles are excluded from the pores of the stationary phase and thus travel faster through the column with the mobile phase, whereas smaller particles penetrate the pores and thus experience a delayed elution from the column and a longer retention time (Fig. 4B) [123]. A recent finding exhibited the capacity of SEC to differentiate different species, including naked mRNA, mRNA-LNP and LNP aggregates in buffer, and to determine the desorption rate of PEG-lipids from siRNA-LNPs in vivo [30,124]. Nevertheless, it should be noted that the stationary phase is prone to interactions with complex biomolecules (e.g., proteins or lipids) or the LNP components, which renders the interpretation of data a complicated task. Besides, the sheer forces during SEC may contribute to alterations of LNP or corona properties.

By coupling SEC to multi-angle light scattering detector (SEC-MALS), characterization of LNPs, can be achieved. It was revealed that the presence of Fab ligands on mRNA-LNPs increased surface hydrophobicity, causing enhanced interparticle association, as indicated by R_g increase [125]. SEC-MALS, with dual columns (with different pore sizes in tandem) and dual-angle light scattering, allowed for chromatographic separation of mRNA-LNPs from blood components, and monitored their degradation kinetics. The LNP disassembly process followed first-order kinetics, with a half-life of 80 min in plasma and 85 min in serum. Within 2 h' incubation, mRNA-LNPs remained relatively stable in serum albumin solution, while mRNA-LNPs exhibited a transition from spherical to elongated morphology during the degradation process in plasma. Moreover, lipid desorption patterns were quantified using liquid chromatography-mass spectrometry (LC-MS)/MS, with a differential desorption order in plasma (ALC-0159 > ALC-0315 > DSPC) compared to serum (ALC-0159 > DSPC > ALC-0315). Notably, even 1 % impurities from 6-((2-hexyldecanoyl)oxy)-N-(6-((2-hexyldecanoyl)oxy)hexyl)-N-(4-hydroxybutyl)hexan-1-aminium (ALC-0315) considerably compromised the stability of mRNA-LNPs in serum, despite minimal effects on size and surface charge [11].

Since isolation approaches for LNPs utilizing size or density fractionation were insufficient for retrieving LNPs from plasma because of the unfavorable overlap with other plasma components. This is unique to clinical LNPs and differentiates them from other nanoparticles that are easier to separate analytically from biofluids. Asymmetric field-flow fractionation (AF4) presents an alternative to SEC for the characterization of LNPs, offering separation by hydrodynamic radius. Unlike SEC that relies on a stationary phase and operates under pressure and sheer, AF4 uses a liquid moving through a thin channel equipped with a membrane and adjustable crossflow, allowing particles to separate based on their diffusion coefficients without the need for crossing through a stationary phase. In combined with MALS, AF4 is considered a viable technique of choice to analyze nanoparticle stability in presence of plasma proteins (e.g., size changes, drug release, protein binding)

[126,127]. However, the unique core structure of RNA-LNP and their relatively labile lipid-monolayer coating are prone to destabilization during the focusing in ***AF4-MALS***, resulting in particle aggregation and sample loss. To improve the performance of AF4-MALS applied to RNA-LNPs, modifications such as replacing the standard AF4 channel with a frit-inlet channel have been implemented, wherein the particles are relaxed hydrodynamically as they are injected. The absence of a focusing step minimizes contact between the particle and the membrane, thus reducing the mentioned artifacts. Through AF4-MALS, the stability of siRNA-LNPs in 10 % human serum and FBS was examined, without significant particle aggregation or destabilization in light scattering fractograms. The increases in R_g mode of 4-6 nm and shifts in retention time indicated the formation of protein corona [128]. Further, Liu et al. developed a ultrafast affinity-based magnetic isolation workflow and exhibited high specificity, recovery rate, and throughput, without compromise of integrity and functionality of the LNPs afterwards [10]. Additionally, combining AF4 with other analytical assay, like small angle X-ray scattering, has been explored to provide further insights into the structural properties of RNA-LNPs, enhancing the comprehensive analysis of their behavior in biological environments [129].

Instead of directly examining the integrity of LNPs, assessing their stability can be achieved by determining the concentration of individual lipid components of the LNP in plasma or serum. Higher concentrations of these components in plasma indicate a higher instability of the corresponding LNP. For instance, the PK profile of ionizable lipid GVS-18-B6 was studied by quantifying its levels in plasma using LC-MS, with a half-life around 30 min after i.v. injection of mRNA-LNPs [130]. Likely, the parent ionizable lipid LC319 and its metabolic products in plasma were analyzed using LC-MS/MS, showing rapid elimination of siRNA-LNPs from mice plasma ($t_{1/2} < 30$ min) after i.v. injection [47]. In another study, LC-MS/MS was used to quantify lipids in plasma and liver, demonstrating that C18-PEG-LNPs resulted in higher plasma exposure and a slower but sustained liver uptake of siRNA compared to identical LNPs containing C14-PEG [131].

3.5. Other fluorescence methods

Fluorescent labeling is a powerful, non-invasive technique that provides high sensitivity and selectivity for real-time monitoring and visualization of LNPs behavior and distribution in biological systems. It enables precise tracking the spatial location and kinetics of RNA-LNPs. Fluorescent RNA-LNPs can be synthesized either by modifying the lipids with fluorescent molecules, encapsulation of fluorescent dyes in the lipid composition or the use of fluorescently labeled nucleic acids. The choice of dye and labeling density can influence the properties of LNPs and thus requires careful optimization of the labeling process [132]. Lipophilic dyes with hydrophobic chains, such as DiI, DiO, DiD and DiR, can be integrated into the hydrophobic lipid segments of LNPs [133]. Chander et al. incorporated DiD-C18 into mRNA-LNPs and measured the DiD fluorescence intensity from blood samples at excitation (Ex)/emission (Em) wavelengths of 644/663 nm. This approach allowed for the assessment of mRNA-LNPs circulation time by normalizing the fluorescence intensity at various time points against the initial mean fluorescence intensity after i.v. administration. Using this assay, DiD-labeled mRNA-LNPs exhibited a circulation half-life of 0.26 h [2]. Similarly, DiO and DiR have been used to localize the distribution of mRNA-LNPs in mice [132]. Note that the fluorescent dye molecules can leak from the LNPs over time and transfer to proteins or cell membranes, especially in complex biological environments [88]. As an alternative approach, lipid component and/or RNA cargo can be fluorescently labeled [49,75]. For instance, siRNA-LNPs were formulated with Cy7-labeled DSPE-PEG and Dy677-labeled siRNA to monitor the circulation of both PEG-lipid and siRNA cargo in mice. Compared to the half-life measured by siRNA fluorescence, the blood half-life of LNPs measured by PEG-lipid fluorescence was extended. This difference was attributed to PEG-lipid association with lipid-rich domains on extracellular vesicles and plasma proteins, leading to prolonged blood circulation [32]. This is in line with the findings from Mui et al., where a longer $t_{1/2}$ was observed by measuring radiolabeled PEG-lipid compared to MC3 [30]. This study well demonstrated that the structural stability (e.g., circulation half-life) of RNA-LNPs is likely to vary when individual lipid components are tracked.

Dual-labeling is widely used to examine the stability, particularly the integrity, of RNA-LNPs, often in combination with Förster Resonance Energy Transfer (FRET). FRET measures the transfer of energy from a donor fluorophore to an acceptor fluorophore through dipole-dipole interaction. The energy transfer efficiency highly depends on the distance between the donor and acceptor molecules (1-10 nm). When the distance increases, the energy transfer efficiency decreases, resulting in increased fluorescence from the donor fluorophore. For example, the dissociation rate of DOPE from siRNA-LNPs in mouse plasma was determined using (donor) NBD-DOPE and (acceptor) LRB-DOPE. When these lipids are in closely associated within the LNP, the fluorescence of NBD is quenched by LRB; while the NBD fluorescence intensity increases when the lipids dissociate. By quantifying the NBD fluorescence at 530 nm, the dissociation $t_{1/2}$ was determined around 4.9 h [31]. The stability of RNA-LNPs can also be assessed by examining the RNA cargo for pre-release, leakage, loss of structural integrity, morphology changes and degradation [106]. In another approach, a FRET pair of Cy5 (donor) and DiR (acceptor) was used to monitor the biodistribution and integrity of mRNA-LNPs (Fig. 4C). When Cy5-labeled luciferase mRNA and DiR-labeled ionizable lipid are in close proximity, the Cy5 fluorescence decreases as the energy transfer to DiR. An increase in Cy5 fluorescence indicates mRNA release from LNPs, with a robust Cy5 signal reflecting substantial release of Cy5-mRNA following systemic injection in mice [134]. Likewise, by encapsulating Cy5-labeled mRNA into rhodamine-labeled LNPs, their stability in culture medium was evaluated using the fluorescence ratio between Cy5 (acceptor) and rhodamine (donor) [10]. Alternatively, Alabi et al. utilized siRNA labeled with AF594 (donor) or AF647 siRNA (acceptor) before encapsulation into LNPs at equimolar ratios. The FRET signal, measured as the ratio of the flputrescence intensities at 690/620 nm, provides insights into the integrity of siRNA LNPs. A FRET signal near 1 indicates an complete disassembly of siRNA-LNPs. This assay is advantageous for high throughput screening of lipids as it does not require the vehicles labeling. Using this assay, they examined the extracellular and intracellular integrity of LNP [135,136].

Fluorescent labeling is a sensitive, specific and non-destructive technique for real-time monitoring of LNPs. But it has limitations in long-term and deep tissue imaging, and also carries the risk, for example, the labeling method requires a sophisticated modification of nanoparticle surface, and the functional groups may affect the interactions between nanoparticles and biological systems or the LNP itself.

3.6. Radioactive labeling

Radioisotope tracing technology, despite concerns regarding the handling of radioactivity, remains a highly sensitive and quantitative method to study the pharmacokinetics and biodistribution of LNPs in vivo. It leverages the tracking of radioactive tracers, such as ^{14}C and ^{3}H, to provides detailed insights into the distribution and fate of nanoparticles after administration (Fig. 4D). Van der Meel et al. utilized ***^{14}C***-DSPC to track siRNA-LNPs after systemic injection, and determined the elimination half-life of 4.63 h using ultra-performance liquid chromatography (UPLC) equipped with a photodiode array detector [137]. ***^{3}H***-labeled cholesteryl hexadecyl ether (CHE) is non-exchangeable and non-metabolizable, and has been used as a marker for siRNA-LNPs. In mouse plasma, ^{3}H-CHE remained in the LNP fractions for over 8 h, while an elimination half-life of siRNA-LNPs was found around 4.55 h [137]. Since ^{3}H-CHE is a stable radioactive label, other radiolabeling lipids, like

^{3}H-PEG-DSG, ^{3}H-PEG-DMG, ^{14}C-DSPC and ^{14}C-DLin-MC3-DMA, were incorporated into siRNA LNPs to measure their dissociation rates respectively, allowing to evaluate the stability of LNPs in mouse plasma [39]. ^{3}H-PEG-DMG dissociated from siRNA-LNP (45 nm) at a significantly faster rate than for larger LNP (80 nm), with a half-time around 1.1 h and 1.7 h, respectively. This is in line with the dissociation rate in case of ^{14}C-DSPC and ^{14}C-DLin-MC3-DMA from siRNA-LNPs [31]. Dual labeling of ^{14}C-MC3 and ^{3}H-PEG-C18 were incorporated into siRNA-LNPs to study their pharmacokinetic in mice, with the clearance $t_{1/2}$ of 4.0 h (^{14}C-MC3) and 4.60 h (^{3}H-PEG-C18) following i.v. injection. This approach allows for investigation into the desorption rate of PEG-lipids as well as their influence on the PK and PD of siRNA-LNPs by analyzing the ^{3}H/^{14}C ratio in blood or plasma [30]. Alternatively, released ***^{2}H***-cholesterols has been used to quantify mRNA-LNPs in plasma and tissue, as deuterium-labeled cholesterols are relatively stable within the LNP bilayer, providing another method for LNPs tracking and evaluation [88].

Instead of directly coupling radionuclide with lipids, metallic radionuclides, such as ^{64}Cu and ^{89}Zr, can be attached to the LNPs using chelators. An early study demonstrated positron emission tomography-computed tomography (PET-CT) imaging as a non-invasive method to monitor the trafficking of a model mRNA vaccine to draining lymph nodes in cynomolgus macaques. In this study, DyLight 680-labeled oligos complementary to the 3′-UTR of the mRNA were used for near-IR imaging, while the divalent metal chelator 1,4,7,10-tetraazacyclododecane-1,4,7,10-tetraacetic acid (DOTA) was conjugated to the NeutrAvidin protein core for whole-body PET-CT [138]. With this approach, Buckley et al. incorporated DSPC-DOTA into mRNA-LNPs and quantitatively tracked ^{64}Cu-loaded DOTA-LNPs in both mice and rhesus macaques using PET imaging [139]. Nevertheless, the incorporation of chelators will influence LNP properties to a much stronger extend than ^{14}C and ^{3}H labelling, but are often easier to apply.

Compared to fluorescent labeling, radiotracing offers unique advantages for quantitative in vivo imaging of nanoparticles. Radiotracing minimizes issues related to tissue background or permeability that can affect fluorescent signals and provides dynamic imaging capabilities, making it ideal for tracking particles in deep tissues of large animals. Nevertheless, the applied doses are significantly lower than therapeutic ones or require the mixing of labeled and non-labeled LNPs to achieve comparable doses. Other limitations are a lower spatial resolution compared the fluorescence in vivo and the complex requirements for radioactive labelling, handling, and imaging.

3.7. Other techniques

Cryogenic electron microscopy (cryo-EM) is most commonly used to visualize LNPs, including shape, size, and internal structure (differences in lipid density) at a high resolution [140]. Following the structure of siRNA-LNPs demonstrated by Cullis and colleagues, the scattering density distribution of mRNA-LNPs was also revealed by cryo-EM [83,141]. Note that the observed scattering contrast at different areas of the LNP does only reflect on the local density of lipids but cannot provide information on molecular organization of individual components. In general, the wide adoption of cryo-EM for RNA-LNPs characterization faces several obstacles, such as high costs, limited accessibility, intricate sample preparation and data analysis [142]. Moreover, the inherent EM micrograph contrast limitations - arising from minor electron density differences between amphiphiles and water – further complicate resolving RNA within lipid component. And background noise, non-uniform illumination and sample preparation artifacts hinder consistent automatic particle identification and analysis [143]. This challenge is magnified in protein containing environments, where molecular crowding and protein interactions obscure LNP features. While several studies showed that RNA-LNPs can be isolated from biofluids before imaging, such as the magnetic isolation or size exclusion assay, this approach carriers risks, such as altering protein corona that may have formed on the LNPs surface and introducing invisible structural changes [10,144]. A full representation of the sample solution, therefore, requires proper sample preparation and a sufficient number of particles measured [145]. Image analysis, often manually or semiautomatically, is time-consuming and limits its potential for high-throughput screening of large LNP libraries, and precise metrics and statistical analysis. Nevertheless, the combination of cryo-EM with complementary bulk techniques, such as DLS, provides valuable information and insights into stability and structural changes of LNPs. In contrast, ***small-angle X-ray scattering*** (SAXS) measures the particles in liquid suspension without sample pre-treatment, even at high-throughput, and provides the spatial distribution and internal structure of the lipid, surfactant, and the bound water in particles [146]. More specifically, it provides direct information about whether ordered lipid or lipid-mRNA structures are present in LNPs, and whether changes in the arrangement of the LNP components occur as a function of physicochemical alterations of the LNP formulation, in addition to size. SAXS, or complemented by other methods (e.g., AF4, cryo-EM, density from solution scattering), can visualize the unique bleb formations characterized by regions of low electron density (blank sections) and high electron density (sections with 2-3 mRNA copies), as well as other subtle structural changes [10,72]. For instance, an increased electrostatic interactions between mRNA and MC3 at pH 4.5 compared to pH 5.7, and a more rough surface of MC3-LNPs and polysarcosine-decorated mRNA-LNPs were detected using SAXS [147]. Since the scattering is proportional to the square of the NP volume, even a relatively small number of aggregates might partially -or fully- cover the scattering features of single LNPs. Therefore, it might be not an optimal tool for highly heterogeneous LNPs, or requires detailed molecular and LNP structural constraints derived from complementary analysis. Alternatively, ***small-angle neutron scattering*** (SANS) is of potential to explore the interactions of LNPs with biological molecules (e.g., peptide, protein), providing information on their partitioning into the lipid matrix and structural rearrangements occurring at the molecular length scale. But due to the limited spatial resolution of SANS in the range of micrometers limits the analysis of individual nanoparticles. Also the structural information is limited and reflects differences in neutron scattering of individual components, the structural information obtained, can be helpful. For example, Gallud et al. investigated the effect of serum proteins on the structure of LNPs using SANS. The parameters obtained from fitted reduced SANS scattering patterns revealed that the LNPs undergo structural changes upon exposure to FBS. Due to insufficient scattering contrast relative to the protein-rich background, the protein corona was not detectable, while the reduction in polar radii and increase in equatorial radii of the mRNA-LNPs was likely attributed to lipid dissociation [148]. A more detailed discussion on these two techniques can be found elsewhere [149].

Serum ***turbidity*** can be used to monitor the stability of mRNA-LNPs qualitatively. A stable formulation is indicated by the absence of serum-induced aggregation and minimal changes in serum turbidity [150]. Exposure to 10 % FBS showed negligible effect on the absorbance at 660 nm (as an indication of turbidity) of mRNA-LNPs, suggesting that mRNA-LNPs remained stable without obvious aggregation [151]. Likewise, Taylor dispersion analysis was used to assess the structural stability of mRNA-LNPs exposed to RNase A, by determining the hydrodynamic diameter [152]. As the concentration of RNA encapsulated within LNPs can be used to estimate the overall concentration of LNPs, Xu et al. determined the plasma clearance of siRNA-LNPs by measuring the siRNA using RT-***PCR***, with a half-life of 0.052 h (DMG-PEG-LNPs) and 0.83 h (DSA-PEG-LNPs) [131].

Nuclear Magnetic Resonance (***NMR***) is a robust quantitative analysis technique for analyzing the diffusion coefficient and surface properties of nanoparticles. By applying a pulsed field gradient, Diffusion-Ordered Spectroscopy (DOSY) NMR measures the self-diffusion of molecules in solution (diffusion coefficient), which can be converted to the hydrodynamic radius allowing the differentiation of compounds according to their size and interaction with the solvent. It is particularly useful for

studying molecular aggregation, supramolecular complexes, and polymer characterization. Besides, conventional NMR (^{1}H, ^{13}C or ^{15}N) can be used to analyze the chemical environment of these atoms. For instance, ^{1}H NMR was used to profile surface PEG and ionizable lipids content and detect changes of surface composition of LNPs in aqueous solution. The internal core (solid-like) is tightly packed with aliphatic groups and has much lower mobility, and thus is not detectable in the conventional NMR analysis [76]. Pulsed gradient spin echo (PGSE) NMR can overcome these limitations offering a quantitative, label-free and real-time method to study PEG shedding kinetics in rat serum. By measuring the self-diffusion coefficient of PEG-lipid in rat serum with a high-resolution NMR probe, it was found that PEG-lipids with longer tail (linoleyl-C18, oleyl-C18) shed slower than those with shorter tail (linoleyl-C14, oleyl-C14). Notably, PEG was not cleaved from its lipid anchor in rat serum, and no lipoprotein association was found in the formulations containing either linoleyl-C18 or oleyl-C18 (Fig. 4E) [105]. This method, indeed, is more appropriate to predict trends than establishing absolute in vivo PEG-lipid shedding rates.

Zhang et al. used quartz crystal microbalance with dissipation monitoring (QCM-D) to understand the interactions between LNPs and proteins (e.g., ApoE). QCM-D is highly sensitive to changes in the interfacial viscoelastic properties and mass-uptake in situ at a high temporal resolution (~1 s). It detects shifts in the frequency and dissipation of an oscillating quartz crystal to provide insights into these interactions. The larger frequency shift for LNP corresponds to increased ApoE adsorption to DOPE-LNPs than DSPC-LNPs. Furthermore, the smaller dissipation shift for a given frequency shift indicated a more rigid coupling between ApoE and LNPs. However, its effectiveness in assessing the stability of RNA-LNPs remains to be further investigated [63].

4. PEG alternatives for an improvement of LNP stability

Since the interaction of LNPs with serum components as well as the steric stabilization requires the use of polymer lipid conjugates, such as PEGylated lipids. PEGylation has been intensively explored as a gold standard to shield nanoparticles from the immune system, reduce protein adsorption, prolong circulation time and improve therapeutic efficacy of RNA-LNPs. As reviewed elsewhere, increasing evidence underscore concerns regarding the common use of PEGylated lipids, particularly when repeated administration or a precise control of immune responses is required [33,40,153–161]. Tremendous efforts have been made to develop PEG replacements [162,163].

Polysarcosine. Polysarcosine (pSar) is emerging as a most promising alternative to PEG in nanomedicine, particularly in the field of RNA delivery [164,165]. As a polypeptoid derived from the endogenous amino acid sarcosine (methyl glycine), pSar offers high biocompatibility, biodegradability and comparable solution properties to PEG (e.g., excellent water solubility, comparable main chain flexibility and low protein affinity) [166–168]. More importantly, pSar has shown stealth-like properties with reduced unspecific interactions with proteins and enables the particles with negligible protein corona, allowing for prolonged circulation in the bloodstream and low liver accumulation [77,169,170]. In our previous studies, pSar-lipids have been utilized to synthesize PEG-free RNA-LNPs. Preclinical research at BioNTech has demonstrated that pSar-based formulations have shown lower immunogenicity and a reduced risk of immune responses compared to their PEG counterparts, while RNA expression remains the same compared to PEGylated lipids at earlier time points and is even improved above 24 h [41]. The structure-activity relationship observed with PEG-lipids also applies to pSar-lipids. For instance, increasing the pSar chain length or anchor lipid length, or increasing the pSar-lipid content within lipid formulations, can prolong the circulation time of particles. This, however, results in reduced cytosolic RNA delivery efficiency [14,41,147]. SAXS studies indicate that an enhanced surface roughness of pSar-LNPs facilitates the delivery to hard-to-transfect cells (e.g., primary immune cells) compared to the identical mRNA-LNPs containing PEG [14,147]. The potential of pSar-lipids in RNA-LNP formulations has been recognized by other researchers, particularly for their comparable shielding effect and superior safety profile compared to PEG-lipids [171]. Following i.v. injection, mRNA delivery efficiency to the liver and spleen was enhanced by using pSar-lipids with shorter hydrophobic tails, and increasing the pSar chain length (higher desorption rate) resulted in a significant preference for mRNA delivery to the liver [172]. Further research is needed to fully understand the potential benefits of pSar as stealth polymer.

Poly(2-oxazoline)s. Poly(2-oxazoline)s (POx) has also seen considerable attention for the design of LNPs, with specific attention on poly(2-methyl-2-oxazoline) (PMeOx) and poly(2-ethyl-2-oxazoline) (PEtOx) as stealth polymers [173–175]. These polymers exhibit comparable physicochemical properties (e.g., non-ionic character, broad solubility in hydrophilic and lipophilic solvents, high flexibility of the main chain) compared to PEG [176,177]. Recent studies have demonstrated that liposomes containing DSPE-PEG, DSPE-PMOx-DSPE or DSPE-PEtOx exhibited prolonged circulation time, indicating the potential of POx as an alternative to PEG for enhancing the longevity of particles in the bloodstream [178]. The use of POx-lipid has also been explored in mRNA-LNPs regarding the in vivo protein production [179]. These studies suggest that POx-lipid can be effectively used in RNA delivery systems, though the relationship between the structure of POx-lipid and its shielding effect remains unclear. Despite these promising findings, the toxicity of POx in vivo and at the gene level is still not well understood. While POx has shown good biocompatibility at the cellular level, more research is needed to fully assess its safety and efficacy in vivo, particularly in the context of genetic material delivery [180,181].

Poly(vinyl pyrrolidone). Poly(N-vinyl pyrrolidone) (PNVP), one of the oldest stealth-polymers, has shown promising results for liposome decoration. Comparable stealth properties was found in siRNA lipoplexes grafted with DSPE-$PNVP_{30}$, with comparable gene silencing efficiency and lower immune response ABC effect after both the first and second injection in mice, compared to DSPE-PEG lipoplexes [182]. This suggests that PNVP can be a viable alternative to PEG for enhancing the stability and efficacy of RNA delivery systems. Additionally, they explored the use of amphiphilic poly(*N*-methyl-N-vinylacetamide) (PNMVA) derivatives in lipid-based siRNA delivery. Incorporation of 15 % DSPE-$PNMVA_{24}$ into lipoplexes strongly limited the formation of a protein corona, indicating good stealth properties comparable to those provided by 15 % DSPE-PEG. Unlike DSPE-PEG, surface coating with DSPE-$PNMVA_{24}$ did not impair the cytosolic delivery of siRNA. In vivo study in mice revealed that DSPE-$PNMVA_{24}$ lipoplexes had an extended circulation time and limited liver accumulation, suggesting a reduced ABC effect following repeated injections, highlighting their biocompatibility and potential for safe, repeated use. Importantly, these lipoplexes did not trigger a systemic pro-inflammatory immune response. Moreover, siRNA-LNPs containing 2.5 mol% DSPE-PNMVA showed an increase in particle concentration and a decrease in total mean particle size after being exposed to FBS for 2 h, indicating a limited protein corona formation and excellent stealth properties [183]. However, further studies are needed to fully understand how PNMVA-lipids alter the performance of grafted RNA-LNPs in vivo, thereof demonstrating the full potential of PNMVA as a PEG-free alternative in the development of RNA delivery systems.

Zwitterionic polymers. Zwitterionic polymers have gained significant recognition for their biocompatibility and antifouling properties, raising promise for a use as PEG substitute in various biomedical applications. Among them, poly(2-methyacryloyloxyethyl phosphorylcholine) (***PMPC***) stands out due to its structural design, which mimics that of the cell membranes. The phosphorylcholine group in the MPS side forms an excellent hydration layer, and exhibits excellent resistance to non-specific protein adsorption, cell adhesion and blood coagulation [184–186]. Therefore, PMPC-lipid coating can significantly reduce protein adsorption in human plasma and blood. In addition, PMPC-LNPs

did not activate inflammatory responses or induce cell mortality, supporting their use in PEG-free LNPs [187]. Although PMPC has shown a high protein resistance, it cannot be considered a stealth polymer. Battaglia and coworkers have nicely shown in various studies that PMPC-decorated polymersomes bind to the scavenger receptor class B member 1 (SRB1) and scavenger receptor class B member 3 (CD36) with high affinity. The high-affinity interactions of PMPC with such receptors are attributed to the phosphorylcholine (PC) groups present in the PMPC chains, which trigger their immediate internalization into cells through endocytosis [188,189].

As another zwitterion, poly(carboxybetaine) (***PCB***) is hydrophilic polymer known for its robust stealth properties and no polymer-specific antibodies production [190]. PCB modification on siRNA lipoplexes has been shown to prevent protein adsorption, enhance stability and avoid ABC phenomenon associated with PEGylation. PCB coatings not only extend blood circulation time but also enhance tumor accumulation of lipoplexes in vivo [191]. Further, a charge-switchable ethylenediamine-based polycarboxybetaine zwitterion (PGlu(DET-Car)) has been developed for decorating siRNA-LNPs. These grafted LNPs exhibited prolonged circulation time in the blood and increased tumor accumulation by selectively switching to a cationic charge in response to the acidic pH of cancerous tissues, enabling more effective interaction with anionic components of the tumor microenvironment [192,193].

5. Conclusion and perspectives

LNPs containing RNA are revolutionizing the way a plethora of diseases is treated. To fully understand and realize their full therapeutic potential for cell-specific RNA delivery in patients, RNA-LNPs must possess the required stability to reach their target site, while enabling RNA translocation into the cytosol upon endocytosis to elicit the desired therapeutic response. Within the complex and dynamic physiological environment of the body, finding the appropriate balance between stability in circulation and efficient RNA release inside cells represents a major task for the development of lipid-based nanoparticles. Although several methods to improve the stability of LNPs are discussed in literature, our fundamental understanding of factors governing internal structure and stability in biological fluids is highly limited and remains descriptive correlating differences in LNP composition with a biological readout. Adjustments of individual components, such as polymer-lipid conjugates, ionizable lipids, helper lipids or cholesterol, alter circulation times, biodistribution and efficacy of RNA delivery. For example, PEGylation has proven effective in enhancing circulation time and improving integrity of RNA-LNPs. But the use of PEGylated lipids is also associated with several drawbacks (e.g., ABC phenomenon, storage disease). As a solution, PEG-free RNA-LNP formulations are being explored to maximize therapeutic efficacy and minimize safety concerns. However, the interactions of LNPs with biological systems in a realistic physiological context is still poorly understood. There is a clear need for more robust and reliable methods to monitor the behavior of LNPs in physiological settings. While several analytical methods enable the LNP characterization in biological fluids (e.g., full serum/plasma or full blood), the use of multiangle DLS, F(*C*)CS and NTA is surprisingly highly limited in the field. We would like to advocate for a more regular implementation of such techniques in the development process of nanomedicines and in particular for lipid-based nanoparticles to improve our understanding of the behavior and performance of LNPs in vivo. We are convinced that this knowledge will become an important cornerstone in unlocking the full potential of RNA-based drugs.

CRediT authorship contribution statement

Heyang Zhang: Writing – review & editing, Writing – original draft, Visualization, Conceptualization. **Matthias Barz:** Writing – review & editing, Writing – original draft, Resources, Project administration, Conceptualization.

Declaration of competing interest

HZ and MB are co-inventors on PCT/EP2023/084377 (HZ & MB) and PCT/EP2018/076633 (MB). MB is scientific advisory board member of Curapath (Paterna, Spain).

Acknowledgement

M.B. acknowledges support by the CRC1066-2/−3 (Project B12) for the development of polysarcosine lipids and formulations thereof.

Data availability

No data was used for the research described in the article.

References

[1] S.A. Dilliard, D.J. Siegwart, Passive, active and endogenous organ-targeted lipid and polymer nanoparticles for delivery of genetic drugs, Nat. Rev. Mater. 8 (2023) 282–300, https://doi.org/10.1038/s41578-022-00529-7.
[2] N. Chander, G. Basha, M.H. Yan Cheng, D. Witzigmann, P.R. Cullis, Lipid nanoparticle mRNA systems containing high levels of sphingomyelin engender higher protein expression in hepatic and extra-hepatic tissues, Mol. Ther. Meth. Clin. Dev. 30 (2023) 235–245, https://doi.org/10.1016/j.omtm.2023.06.005.
[3] M.N. Martinez, Factors influencing the use and interpretation of animal models in the development of parenteral drug delivery systems, AAPS Journal 13 (2011) 632–649, https://doi.org/10.1208/s12248-011-9303-8.
[4] N. Bertrand, J.C. Leroux, The journey of a drug-carrier in the body: an anatomo-physiological perspective, J. Control. Release 161 (2012) 152–163, https://doi.org/10.1016/j.jconrel.2011.09.098.
[5] D. Witzigmann, J.A. Kulkarni, J. Leung, S. Chen, P.R. Cullis, R. van der Meel, Lipid nanoparticle technology for therapeutic gene regulation in the liver, Adv. Drug Deliv. Rev. 159 (2020) 344–363, https://doi.org/10.1016/j.addr.2020.06.026.
[6] M.Z.C. Hatit, M.P. Lokugamage, C.N. Dobrowolski, K. Paunovska, H. Ni, K. Zhao, D. Vanover, J. Beyersdorf, H.E. Peck, D. Loughrey, M. Sato, A. Cristian, P. J. Santangelo, J.E. Dahlman, Species-dependent in vivo mRNA delivery and cellular responses to nanoparticles, Nat. Nanotechnol. 17 (2022) 310–318, https://doi.org/10.1038/s41565-021-01030-y.
[7] S.A. Dilliard, Q. Cheng, D.J. Siegwart, J. Desimone, On the mechanism of tissue-specific mRNA delivery by selective organ targeting nanoparticles, Proc. Natl. Acad. Sci. 118 (2021) e2109256118, https://doi.org/10.1073/pnas.2109256118/-/DCSupplemental.
[8] M. Barz, W.J. Parak, R. Zentel, Concepts and approaches to reduce or avoid protein Corona formation on nanoparticles: challenges and opportunities, Adv. Sci. (2024), https://doi.org/10.1002/advs.202402935.
[9] A. Akinc, M.A. Maier, M. Manoharan, K. Fitzgerald, M. Jayaraman, S. Barros, S. Ansell, X. Du, M.J. Hope, T.D. Madden, B.L. Mui, S.C. Semple, Y.K. Tam, M. Ciufolini, D. Witzigmann, J.A. Kulkarni, R. Van Der Meel, P.R. Cullis, The Onpattro story and the clinical translation of nanomedicines containing nucleic acid-based drugs, 2025, https://doi.org/10.1038/s41565-019-0591-y.
[10] K. Liu, R. Nilsson, E. Lázaro-Ibáñez, H. Duàn, T. Miliotis, M. Strimfors, M. Lerche, A.R. Salgado Ribeiro, J. Ulander, D. Lindén, A. Salvati, A. Sabirsh, Multiomics analysis of naturally efficacious lipid nanoparticle coronas reveals high-density lipoprotein is necessary for their function, Nat. Commun. 14 (2023), https://doi.org/10.1038/s41467-023-39768-9.
[11] B. Liau, L. Zhang, M.J.Y. Ang, J.Y. Ng, S.B. Suresh, S. Schneider, R. Gudihal, K. H. Bae, Y.Y. Yang, Quantitative analysis of mRNA-lipid nanoparticle stability in human plasma and serum by size-exclusion chromatography coupled with dual-angle light scattering, Nanomedicine 58 (2024), https://doi.org/10.1016/j.nano.2024.102745.
[12] S.T. LoPresti, M.L. Arral, N. Chaudhary, K.A. Whitehead, The replacement of helper lipids with charged alternatives in lipid nanoparticles facilitates targeted mRNA delivery to the spleen and lungs, J. Control. Release 345 (2022) 819–831, https://doi.org/10.1016/j.jconrel.2022.03.046.
[13] Q. Cheng, T. Wei, L. Farbiak, L.T. Johnson, S.A. Dilliard, D.J. Siegwart, Selective organ targeting (SORT) nanoparticles for tissue-specific mRNA delivery and CRISPR–Cas gene editing, Nat. Nanotechnol. 15 (2020) 313–320, https://doi.org/10.1038/s41565-020-0669-6.
[14] D. Bi, C. Wilhelmy, D. Unthan, I.S. Keil, B. Zhao, B. Kolb, R.I. Koning, M. A. Graewert, B. Wouters, R. Zwier, J. Bussmann, T. Hankemeier, M. Diken, H. Haas, P. Langguth, M. Barz, H. Zhang, On the influence of fabrication methods and materials for mRNA-LNP production: from size and morphology to internal structure and mRNA delivery performance in vitro and in vivo, Adv. Healthc. Mater. (2024), https://doi.org/10.1002/adhm.202401252.
[15] M.E. Gindy, B. Feuston, A. Glass, L. Arrington, R.M. Haas, J. Schariter, S. M. Stirdivant, Stabilization of ostwald ripening in low molecular weight amino lipid nanoparticles for systemic delivery of siRNA therapeutics, Mol. Pharm. 11 (2014) 4143–4153, https://doi.org/10.1021/mp500367k.
[16] R. Shi, X. Liu, Y. Wang, M. Pan, S. Wang, L. Shi, B. Ni, Long-term stability and immunogenicity of lipid nanoparticle COVID-19 mRNA vaccine is affected by

particle size, Hum. Vaccin. Immunother. 20 (2024), https://doi.org/10.1080/21645515.2024.2342592.
[17] M. Kamiya, M. Matsumoto, K. Yamashita, T. Izumi, M. Kawaguchi, S. Mizukami, M. Tsurumaru, H. Mukai, S. Kawakami, Stability study of mRNA-lipid nanoparticles exposed to various conditions based on the evaluation between physicochemical properties and their relation with protein expression ability, Pharmaceutics 14 (2022), https://doi.org/10.3390/pharmaceutics14112357.
[18] D.J.A. Crommelin, T.J. Anchordoquy, D.B. Volkin, W. Jiskoot, E. Mastrobattista, Addressing the cold reality of mRNA vaccine stability, J. Pharm. Sci. 110 (2021) 997–1001, https://doi.org/10.1016/j.xphs.2020.12.006.
[19] K. Leppek, G.W. Byeon, W. Kladwang, H.K. Wayment-Steele, C.H. Kerr, A.F. Xu, D.S. Kim, V.V. Topkar, C. Choe, D. Rothschild, G.C. Tiu, R. Wellington-Oguri, K. Fujii, E. Sharma, A.M. Watkins, J.J. Nicol, J. Romano, B. Tunguz, F. Diaz, H. Cai, P. Guo, J. Wu, F. Meng, S. Shi, E. Participants, P.R. Dormitzer, A. Solórzano, M. Barna, R. Das, Combinatorial optimization of mRNA structure, stability, and translation for RNA-based therapeutics, Nat. Commun. 13 (2022), https://doi.org/10.1038/s41467-022-28776-w.
[20] F. Cheng, Y. Wang, Y. Bai, Z. Liang, Q. Mao, D. Liu, X. Wu, M. Xu, Research advances on the stability of mRNA vaccines, Viruses 15 (2023), https://doi.org/10.3390/v15030668.
[21] L. Ai, Y. Li, L. Zhou, W. Yao, H. Zhang, Z. Hu, J. Han, W. Wang, J. Wu, P. Xu, R. Wang, Z. Li, Z. Li, C. Wei, J. Liang, H. Chen, Z. Yang, M. Guo, Z. Huang, X. Wang, Z. Zhang, W. Xiang, D. Sun, L. Xu, M. Huang, B. Lv, P. Peng, S. Zhang, X. Ji, H. Luo, N. Chen, J. Chen, K. Lan, Y. Hu, Lyophilized mRNA-lipid nanoparticle vaccines with long-term stability and high antigenicity against SARS-CoV-2, Cell Discov 9 (2023), https://doi.org/10.1038/s41421-022-00517-9.
[22] R. Lball, P. Bajaj, K.A. Whitehead, Achieving long-term stability of lipid nanoparticles: examining the effect of pH, temperature, and lyophilization, Int. J. Nanomedicine 12 (2017) 305–315, https://doi.org/10.2147/IJN.S123062.
[23] L. Zhang, K.R. More, A. Ojha, C.B. Jackson, B.D. Quinlan, H. Li, W. He, M. Farzan, N. Pardi, H. Choe, Effect of mRNA-LNP components of two globally-marketed COVID-19 vaccines on efficacy and stability, NPJ Vaccines 8 (2023), https://doi.org/10.1038/s41541-023-00751-6.
[24] X. Hou, T. Zaks, R. Langer, Y. Dong, Lipid nanoparticles for mRNA delivery, Nat. Rev. Mater. 6 (2021) 1078–1094, https://doi.org/10.1038/s41578-021-00358-0.
[25] V. Kumar, J. Qin, Y. Jiang, R.G. Duncan, B. Brigham, S. Fishman, J.K. Nair, A. Akinc, S.A. Barros, P.V. Kasperkovitz, Shielding of lipid nanoparticles for siRNA delivery: impact on physicochemical properties, cytokine induction, and efficacy, Mol Ther Nucleic Acids 3 (2014) e210, https://doi.org/10.1038/mtna.2014.61.
[26] E. Padín-González, P. Lancaster, M. Bottini, P. Gasco, L. Tran, B. Fadeel, T. Wilkins, M.P. Monopoli, Understanding the role and impact of poly (ethylene glycol) (PEG) on nanoparticle formulation: implications for COVID-19 vaccines, front Bioeng, Biotechnol 10 (2022) 1–16, https://doi.org/10.3389/fbioe.2022.882363.
[27] C. Zhao, H. Deng, J. Xu, S. Li, L. Zhong, L. Shao, Y. Wu, X.J. Liang, Sheddable PEG-lipid to balance the contradiction of PEGylation between long circulation and poor uptake, Nanoscale 8 (2016) 10832–10842, https://doi.org/10.1039/c6nr02174c.
[28] D. Pozzi, V. Colapicchioni, G. Caracciolo, S. Piovesana, A.L. Capriotti, S. Palchetti, S. De Grossi, A. Riccioli, H. Amenitsch, A. Laganà, Effect of polyethyleneglycol (PEG) chain length on the bio-nano- interactions between PEGylated lipid nanoparticles and biological fluids: from nanostructure to uptake in cancer cells, Nanoscale 6 (2014) 2782–2792, https://doi.org/10.1039/c3nr05559k.
[29] A. Sarode, Y. Fan, A.E. Byrnes, M. Hammel, G.L. Hura, Y. Fu, P. Kou, C. Hu, F. I. Hinz, J. Roberts, S.G. Koenig, K. Nagapudi, C.C. Hoogenraad, T. Chen, D. Leung, C.-W. Yen, Predictive high-throughput screening of PEGylated lipids in oligonucleotide-loaded lipid nanoparticles for neuronal gene silencing, 2022, https://doi.org/10.1039/d1na00712b.
[30] B.L. Mui, Y.K. Tam, M. Jayaraman, S.M. Ansell, X. Du, Y. Yi C. Tam, P.J.C. Lin, S. Chen, J.K. Narayanannair, K.G. Rajeev, M. Manoharan, A. Akinc, M.A. Maier, P. Cullis, T.D. Madden, M.J. Hope, Influence of Polyethylene Glycol Lipid Desorption Rates on Pharmacokinetics and Pharmacodynamics of siRNA Lipid Nanoparticles, Mol Ther Nucleic Acids 2 (2013), https://doi.org/10.1038/mtna.2013.66.
[31] S. Chen, Y.Y.C. Tam, P.J.C. Lin, M.M.H. Sung, Y.K. Tam, P.R. Cullis, Influence of particle size on the in vivo potency of lipid nanoparticle formulations of siRNA, J. Control. Release 235 (2016), https://doi.org/10.1016/j.jconrel.2016.05.059.
[32] L.E. Waggoner, K.F. Miyasaki, E.J. Kwon, Analysis of PEG-lipid anchor length on lipid nanoparticle pharmacokinetics and activity in a mouse model of traumatic brain injury, Biomater. Sci. 11 (2023) 4238–4253, https://doi.org/10.1039/d2bm01846b.
[33] Y. Lee, M. Jeong, G. Lee, J. Park, H. Jung, S. Im, H. Lee, Development of lipid nanoparticle formulation for the repeated administration of mRNA therapeutics, Biomater Res 28 (2024), https://doi.org/10.34133/bmr.0017.
[34] C. Masson, M. Garinot, N. Mignet, B. Wetzer, P. Mailhe, D. Scherman, M. Bessodes, pH-sensitive PEG lipids containing orthoester linkers: new potential tools for nonviral gene delivery, J. Control. Release 99 (2004) 423–434, https://doi.org/10.1016/j.jconrel.2004.07.016.
[35] F. Coelho, L.M. Salonen, B.F.B. Silva, Hemiacetal-linked pH-sensitive PEG-lipids for non-viral gene delivery, New J. Chem. 46 (2022) 15414–15422, https://doi.org/10.1039/d2nj02217f.
[36] Y. Fang, J. Xue, S. Gao, A. Lu, D. Yang, H. Jiang, Y. He, K. Shi, Cleavable PEGylation: a strategy for overcoming the "PEG dilemma" in efficient drug delivery, Drug Deliv. 24 (2017) 22–32, https://doi.org/10.1080/10717544.2017.1388451.
[37] L. Shi, J. Zhang, M. Zhao, S. Tang, X. Cheng, W. Zhang, W. Li, X. Liu, H. Peng, Q. Wang, Effects of polyethylene glycol on the surface of nanoparticles for targeted drug delivery, Nanoscale 13 (2021) 10748, https://doi.org/10.1039/d1nr02065j.
[38] J.B. Lee, K. Zhang, Y.Y.C. Tam, J. Quick, Y.K. Tam, P.J. Lin, S. Chen, Y. Liu, J. K. Nair, I. Zlatev, K.G. Rajeev, M. Manoharan, P.S. Rennie, P.R. Cullis, A Glu-urea-Lys ligand-conjugated lipid nanoparticle/siRNA system inhibits androgen receptor expression in vivo, Mol Ther Nucleic Acids 5 (2016) e348, https://doi.org/10.1038/mtna.2016.43.
[39] S. Chen, Y.Y.C. Tam, P.J.C. Lin, A.K.K. Leung, Y.K. Tam, P.R. Cullis, Development of lipid nanoparticle formulations of siRNA for hepatocyte gene silencing following subcutaneous administration, J. Control. Release 196 (2014) 106–112, https://doi.org/10.1016/j.jconrel.2014.09.025.
[40] R. Tenchov, J.M. Sasso, Q.A. Zhou, PEGylated lipid nanoparticle formulations: immunological safety and efficiency perspective, Bioconjug. Chem. 34 (2023) 941–960, https://doi.org/10.1021/acs.bioconjchem.3c00174.
[41] S.S. Nogueira, A. Schlegel, K. Maxeiner, B. Weber, M. Barz, M.A. Schroer, C. E. Blanchet, D.I. Svergun, S. Ramishetti, D. Peer, P. Langguth, U. Sahin, H. Haas, Polysarcosine-functionalized lipid nanoparticles for therapeutic mRNA delivery, ACS Appl. Nano Mater. 3 (2020) 10634–10645, https://doi.org/10.1021/acsanm.0c01834.
[42] M. Sedic, J.J. Senn, A. Lynn, M. Laska, M. Smith, S.J. Platz, J. Bolen, S. Hoge, A. Bulychev, E. Jacquinet, V. Bartlett, P.F. Smith, Safety Evaluation of Lipid Nanoparticle–Formulated Modified mRNA in the Sprague-Dawley Rat and Cynomolgus Monkey, Vet. Pathol. 55 (2018) 341–354, https://doi.org/10.1177/0300985817738095.
[43] S. Sabnis, E.S. Kumarasinghe, T. Salerno, C. Mihai, T. Ketova, J.J. Senn, A. Lynn, A. Bulychev, I. McFadyen, J. Chan, Ö. Almarsson, M.G. Stanton, K.E. Benenato, A novel amino lipid series for mRNA delivery: improved endosomal escape and sustained pharmacology and safety in non-human primates, Mol. Ther. 26 (2018) 1509–1519, https://doi.org/10.1016/j.ymthe.2018.03.010.
[44] M.C.P. Mendonca, A. Kont, P.S. Kowalski, C.M. O'Driscoll, Design of lipid-based nanoparticles for delivery of therapeutic nucleic acids, Drug Discov. Today 28 (2023) 1–17.
[45] D. Sun, Z.R. Lu, Structure and function of cationic and Ionizable lipids for nucleic acid delivery, Pharm. Res. 40 (2023) 27–46, https://doi.org/10.1007/s11095-022-03460-2.
[46] A.M. Jörgensen, R. Wibel, A. Bernkop-Schnürch, Biodegradable cationic and Ionizable cationic lipids: a roadmap for safer pharmaceutical excipients, Small 19 (2023), https://doi.org/10.1002/smll.202206968.
[47] M.A. Maier, M. Jayaraman, S. Matsuda, J. Liu, S. Barros, W. Querbes, Y.K. Tam, S. M. Ansell, V. Kumar, J. Qin, X. Zhang, Q. Wang, S. Panesar, R. Hutabarat, M. Carioto, J. Hettinger, P. Kandasamy, D. Butler, K.G. Rajeev, B. Pang, K. Charisse, K. Fitzgerald, B.L. Mui, X. Du, P. Cullis, T.D. Madden, M.J. Hope, M. Manoharan, A. Akinc, Biodegradable lipids enabling rapidly eliminated lipid nanoparticles for systemic delivery of RNAi therapeutics, Mol. Ther. 21 (2013) 1570–1578, https://doi.org/10.1038/mt.2013.124.
[48] J. Couture-Senécal, G. Tilstra, O.F. Khan, Engineering ionizable lipids for rapid biodegradation balances mRNA vaccine efficacy and tolerability, BioRxiv (2024), https://doi.org/10.1101/2024.08.02.606386.
[49] S.C. Semple, A. Akinc, J. Chen, A.P. Sandhu, B.L. Mui, C.K. Cho, D.W.Y. Sah, D. Stebbing, E.J. Crosley, E. Yaworski, I.M. Hafez, J.R. Dorkin, J. Qin, K. Lam, K. G. Rajeev, K.F. Wong, L.B. Jeffs, L. Nechev, M.L. Eisenhardt, M. Jayaraman, M. Kazem, M.A. Maier, M. Srinivasulu, M.J. Weinstein, Q. Chen, R. Alvarez, S. A. Barros, S. De, S.K. Klimuk, T. Borland, V. Kosovrasti, W.L. Cantley, Y.K. Tam, M. Manoharan, M.A. Ciufolini, M.A. Tracy, A. De Fougerolles, I. MacLachlan, P. R. Cullis, T.D. Madden, M.J. Hope, Rational design of cationic lipids for siRNA delivery, Nat. Biotechnol. 28 (2010) 172–176, https://doi.org/10.1038/nbt.1602.
[50] K. Hashiba, Y. Sato, M. Taguchi, S. Sakamoto, A. Otsu, Y. Maeda, T. Shishido, M. Murakawa, A. Okazaki, H. Harashima, Branching Ionizable lipids can enhance the stability, Fusogenicity, and functional delivery of mRNA, Small Science 3 (2023), https://doi.org/10.1002/smsc.202200071.
[51] K.A. Hajj, R.L. Ball, S.B. Deluty, S.R. Singh, D. Strelkova, C.M. Knapp, K. A. Whitehead, Branched-tail lipid nanoparticles potently deliver mRNA in vivo due to enhanced ionization at endosomal pH, Small 15 (2019), https://doi.org/10.1002/smll.201805097.
[52] I. Ermilova, J. Swenson, Ionizable lipids penetrate phospholipid bilayers with high phase transition temperatures: perspectives from free energy calculations, Chem. Phys. Lipids 253 (2023), https://doi.org/10.1016/j.chemphyslip.2023.105294.
[53] O.S. Fenton, K.J. Kauffman, R.L. McClellan, E.A. Appel, J.R. Dorkin, M.W. Tibbitt, M.W. Heartlein, F. DeRosa, R. Langer, D.G. Anderson, Bioinspired alkenyl amino alcohol Ionizable lipid materials for highly potent in vivo mRNA delivery, Adv. Mater. 28 (2016) 2939–2943, https://doi.org/10.1002/adma.201505822.
[54] S. Dehghani-Ghahnaviyeh, M. Smith, Y. Xia, A. Dousis, A. Grossfield, S. Sur, Ionizable amino lipids distribution and effects on DSPC/cholesterol membranes: implications for lipid nanoparticle structure, J. Phys. Chem. B 127 (2023) 6928–6939, https://doi.org/10.1021/acs.jpcb.3c01296.
[55] M. Schlich, R. Palomba, G. Costabile, S. Mizrahy, M. Pannuzzo, D. Peer, P. Decuzzi, Cytosolic delivery of nucleic acids: the case of ionizable lipid nanoparticles, Bioeng Transl Med 6 (2021), https://doi.org/10.1002/btm2.10213.

[56] A.K.K. Leung, Y.Y.C. Tam, S. Chen, I.M. Hafez, P.R. Cullis, Microfluidic mixing: a general method for encapsulating macromolecules in lipid nanoparticle systems, J. Phys. Chem. B 119 (2015) 8698–8706, https://doi.org/10.1021/acs.jpcb.5b02891.
[57] S. Wang, X. Wei, X. Sun, C. Chen, J. Zhou, G. Zhang, H. Wu, B. Guo, L. Wei, A novel therapeutic strategy for cartilage diseases based on lipid nanoparticle-RNAi delivery system, Int. J. Nanomedicine 13 (2018) 617–631, https://doi.org/10.2147/IJN.S142797.
[58] K.J. Kauffman, J.R. Dorkin, J.H. Yang, M.W. Heartlein, F. Derosa, F.F. Mir, O. S. Fenton, D.G. Anderson, Optimization of lipid nanoparticle formulations for mRNA delivery in vivo with fractional factorial and definitive screening designs, Nano Lett. 15 (2015) 7300–7306, https://doi.org/10.1021/acs.nanolett.5b02497.
[59] R. Pattipeiluhu, Y. Zeng, M.M.R.M. Hendrix, I.K. Voets, A. Kros, T.H. Sharp, Liquid crystalline inverted lipid phases encapsulating siRNA enhance lipid nanoparticle mediated transfection, Nat. Commun. 15 (2024), https://doi.org/10.1038/s41467-024-45666-5.
[60] D.N. Zimmer, F. Schmid, G. Settanni, Ionizable cationic lipids and helper lipids synergistically contribute to RNA packing and protection in lipid-based nanomaterials, J. Phys. Chem. B (2024), https://doi.org/10.1021/acs.jpcb.4c05057.
[61] J. Lu, T. Jiang, X. Li, S. Tan, Y. Zhang, H. Gu, L. Chen, J. Guo, R. Yu, J. Zang, D. Ouyang, H. Yu, H. Yao, M. Qiu, J. Lin, Dual ethanolamine head groups in Ionizable lipids facilitate phospholipid-free stable nanoparticle formulation for augmented and safer mRNA delivery, BioRxiv (2023), https://doi.org/10.1101/2023.10.13.562139.
[62] I. Ermilova, J. Swenson, DOPC: versus DOPE as a helper lipid for gene-therapies: molecular dynamics simulations with DLin-MC3-DMA, Phys. Chem. Chem. Phys. 22 (2020) 28256–28268, https://doi.org/10.1039/d0cp05111j.
[63] R. Zhang, R. El-Mayta, T.J. Murdoch, C.C. Warzecha, M.M. Billingsley, S. J. Shepherd, N. Gong, L. Wang, J.M. Wilson, D. Lee, M.J. Mitchell, Helper lipid structure influences protein adsorption and delivery of lipid nanoparticles to spleen and liver, Biomater. Sci. 9 (2021) 1449–1463, https://doi.org/10.1039/d0bm01609h.
[64] M. Kawaguchi, M. Noda, A. Ono, M. Kamiya, M. Matsumoto, M. Tsurumaru, S. Mizukami, H. Mukai, S. Kawakami, Effect of cholesterol content of lipid composition in mRNA-LNPs on the protein expression in the injected site and liver after local Administration in Mice, J. Pharm. Sci. 112 (2023) 1401–1410, https://doi.org/10.1016/j.xphs.2022.12.026.
[65] Y. Sato, Y. Note, M. Maeki, N. Kaji, Y. Baba, M. Tokeshi, H. Harashima, Elucidation of the physicochemical properties and potency of siRNA-loaded small-sized lipid nanoparticles for siRNA delivery, J. Control. Release 229 (2016) 48–57, https://doi.org/10.1016/j.jconrel.2016.03.019.
[66] Y. Eygeris, S. Patel, A. Jozic, G. Sahay, G. Sahay, Deconvoluting lipid nanoparticle structure for messenger RNA delivery, Nano Lett. 20 (2020) 4543–4549, https://doi.org/10.1021/acs.nanolett.0c01386.
[67] A. Medjmedj, A. Ngalle-Loth, R. Clemençon, J. Hamacek, C. Pichon, F. Perche, In Cellulo and in vivo comparison of cholesterol, Beta-Sitosterol and Dioleylphosphatidylethanolamine for lipid nanoparticle formulation of mRNA, Nanomaterials 12 (2022), https://doi.org/10.3390/nano12142446.
[68] K. Paunovska, C.J. Gil, M.P. Lokugamage, C.D. Sago, M. Sato, G.N. Lando, M. Gamboa Castro, A.V. Bryksin, J.E. Dahlman, Analyzing 2000 in vivo drug delivery data points reveals cholesterol structure impacts nanoparticle delivery, ACS Nano 12 (2018) 8341–8349, https://doi.org/10.1021/acsnano.8b03640.
[69] E. Ikonen, Cellular cholesterol trafficking and compartmentalization, Nat. Rev. Mol. Cell Biol. 9 (2008) 125–138. www.nature.com/reviews/molcellbio.
[70] W. Kulig, L. Cwiklik, P. Jurkiewicz, T. Rog, I. Vattulainen, Cholesterol oxidation products and their biological importance, Chem. Phys. Lipids 199 (2016) 144–160, https://doi.org/10.1016/j.chemphyslip.2016.03.001.
[71] K. Paunovska, A.J. Da Silva Sanchez, C.D. Sago, Z. Gan, M.P. Lokugamage, F. Z. Islam, S. Kalathoor, B.R. Krupczak, J.E. Dahlman, Nanoparticles containing oxidized cholesterol deliver mRNA to the liver microenvironment at clinically relevant doses, Adv. Mater. 31 (2019), https://doi.org/10.1002/adma.201807748.
[72] H.M. Dao, K. AboulFotouh, A.F. Hussain, A.E. Marras, K.P. Johnston, Z. Cui, R. O. Williams, Characterization of mRNA lipid nanoparticles by Electron density mapping reconstruction: X-ray scattering with density from solution scattering (DENSS) algorithm, Pharm. Res. 41 (2024) 501–512, https://doi.org/10.1007/s11095-024-03671-9.
[73] M. Cárdenas, R.A. Campbell, M. Yanez Arteta, M.J. Lawrence, F. Sebastiani, Review of structural design guiding the development of lipid nanoparticles for nucleic acid delivery, Curr Opin colloid, Interface Sci. 66 (2023), https://doi.org/10.1016/j.cocis.2023.101705.
[74] Y. Yan, X.Y. Liu, A. Lu, X.Y. Wang, L.X. Jiang, J.C. Wang, Non-viral vectors for RNA delivery, J. Control. Release 342 (2022) 241–279, https://doi.org/10.1016/j.jconrel.2022.01.008.
[75] R. Pattipeiluhu, G. Arias-Alpizar, G. Basha, K.Y.T. Chan, J. Bussmann, T.H. Sharp, M.A. Moradi, N. Sommerdijk, E.N. Harris, P.R. Cullis, A. Kros, D. Witzigmann, F. Campbell, Anionic lipid nanoparticles preferentially deliver mRNA to the hepatic reticuloendothelial system, Adv. Mater. 34 (2022), https://doi.org/10.1002/adma.202201095.
[76] M.M. Wang, C.N. Wappelhorst, E.L. Jensen, Y.C.T. Chi, J.C. Rouse, Q. Zou, Elucidation of lipid nanoparticle surface structure in mRNA vaccines, Sci. Rep. 13 (2023), https://doi.org/10.1038/s41598-023-43898-x.
[77] I. Alberg, S. Kramer, M. Schinnerer, Q. Hu, C. Seidl, C. Leps, N. Drude, D. Möckel, C. Rijcken, T. Lammers, M. Diken, M. Maskos, S. Morsbach, K. Landfester, S. Tenzer, M. Barz, R. Zentel, Polymeric nanoparticles with neglectable protein corona, Small 16 (2020) 1907574, https://doi.org/10.1002/smll.201907574.
[78] R. Pattipeiluhu, S. Crielaard, I. Klein-Schiphorst, B.I. Florea, A. Kros, F. Campbell, Unbiased identification of the liposome protein Corona using Photoaffinity-based Chemoproteomics, ACS Cent. Sci. 6 (2020) 535–545, https://doi.org/10.1021/acscentsci.9b01222.
[79] S. Yeo, H. Lee, J. Lee, H. Lee, H. Mok, Optimization of polyethylene glycol shielding and mannose density on the lipid nanoparticles for efficient delivery to macrophages and spleens, Int. J. Pharm. 662 (2024), https://doi.org/10.1016/j.ijpharm.2024.124540.
[80] K.J. Hassett, J. Higgins, A. Woods, B. Levy, Y. Xia, C.J. Hsiao, E. Acosta, Ö. Almarsson, M.J. Moore, L.A. Brito, Impact of lipid nanoparticle size on mRNA vaccine immunogenicity, J. Control. Release 335 (2021) 237–246, https://doi.org/10.1016/j.jconrel.2021.05.021.
[81] J.B. Simonsen, A perspective on bleb and empty LNP structures, J. Control. Release 373 (2024) 952–961, https://doi.org/10.1016/j.jconrel.2024.07.046.
[82] M.H.Y. Cheng, J. Leung, Y. Zhang, C. Strong, G. Basha, A. Momeni, Y. Chen, E. Jan, A. Abdolahzadeh, X. Wang, J.A. Kulkarni, D. Witzigmann, P.R. Cullis, Induction of bleb structures in lipid nanoparticle formulations of mRNA leads to improved transfection potency, Adv. Mater. 35 (2023), https://doi.org/10.1002/adma.202303370.
[83] J.A. Kulkarni, M.M. Darjuan, J.E. Mercer, S. Chen, R. Van Der Meel, J.L. Thewalt, Y.Y.C. Tam, P.R. Cullis, On the formation and morphology of lipid nanoparticles containing Ionizable cationic lipids and siRNA, ACS Nano 12 (2018) 4787–4795, https://doi.org/10.1021/acsnano.8b01516.
[84] D. Thirumalai, C. Hyeon, ‡ biophysics, RNA and protein folding: common themes and variations, Biochemistry 44 (2005) 39, https://doi.org/10.1021/bi047314.
[85] S. Meulewaeter, G. Nuytten, M.H.Y. Cheng, S.C. De Smedt, P.R. Cullis, T. De Beer, I. Lentacker, R. Verbeke, Continuous freeze-drying of messenger RNA lipid nanoparticles enables storage at higher temperatures, J. Control. Release 357 (2023) 149–160, https://doi.org/10.1016/j.jconrel.2023.03.039.
[86] M.I. Henderson, Y. Eygeris, A. Jozic, M. Herrera, G. Sahay, Leveraging biological buffers for efficient messenger RNA delivery via lipid nanoparticles, Mol. Pharm. 19 (2022) 4275–4285, https://doi.org/10.1021/acs.molpharmaceut.2c00587.
[87] V. Gote, P.K. Bolla, N. Kommineni, A. Butreddy, P.K. Nukala, S.S. Palakurthi, W. Khan, A comprehensive review of mRNA vaccines, Int. J. Mol. Sci. 24 (2023), https://doi.org/10.3390/ijms24032700.
[88] J. Di, Z. Du, K. Wu, S. Jin, X. Wang, T. Li, Y. Xu, Biodistribution and Non-linear Gene Expression of mRNA LNPs Affected by Delivery Route and Particle Size, 2025, https://doi.org/10.1007/s11095-022-03166-5/Published.
[89] J.R. Melamed, S.S. Yerneni, M.L. Arral, S.T. Lopresti, N. Chaudhary, A. Sehrawat, H. Muramatsu, M.-G. Alameh, N. Pardi, D. Weissman, G.K. Gittes, K. A. Whitehead, Ionizable Lipid Nanoparticles Deliver mRNA to Pancreatic β Cells Via Macrophage-Mediated Gene Transfer. https://www.science.org, 2023.
[90] K.A. Hajj, J.R. Melamed, N. Chaudhary, N.G. Lamson, R.L. Ball, S.S. Yerneni, K. A. Whitehead, A Potent Branched-Tail Lipid Nanoparticle Enables Multiplexed mRNA Delivery and Gene Editing In Vivo, 2020, https://doi.org/10.1021/acs.nanolett.0c00596.
[91] E.H. Pilkington, E.J.A. Suys, N.L. Trevaskis, A.K. Wheatley, D. Zukancic, A. Algarni, H. Al-Wassiti, T.P. Davis, C.W. Pouton, S.J. Kent, N.P. Truong, From influenza to COVID-19: lipid nanoparticle mRNA vaccines at the frontiers of infectious diseases, Acta Biomater. 131 (2021) 16–40, https://doi.org/10.1016/j.actbio.2021.06.023.
[92] H. Zhang, J. Vandesompele, K. Braeckmans, S.C. De Smedt, K. Remaut, Nucleic acid degradation as barrier to gene delivery: a guide to understand and overcome nuclease activity, Chem. Soc. Rev. 53 (2023) 317–360, https://doi.org/10.1039/d3cs00194f.
[93] S.G. Huayamares, R. Zenhausern, D. Loughrey, Nanocarriers for inhaled delivery of RNA therapeutics, Curr Res Biotechnol 7 (2024), https://doi.org/10.1016/j.crbiot.2024.100200.
[94] Q. Xu, L.M. Ensign, N.J. Boylan, A. Schön, X. Gong, J.C. Yang, N.W. Lamb, S. Cai, T. Yu, E. Freire, J. Hanes, Impact of surface polyethylene glycol (PEG) density on biodegradable nanoparticle transport in mucus ex vivo and distribution in vivo, ACS Nano 9 (2015) 9217–9227, https://doi.org/10.1021/acsnano.5b03876.
[95] M.P. Lokugamage, D. Vanover, J. Beyersdorf, M.Z.C. Hatit, L. Rotolo, E. S. Echeverri, H.E. Peck, H. Ni, J.K. Yoon, Y.T. Kim, P.J. Santangelo, J.E. Dahlman, Optimization of lipid nanoparticles for the delivery of nebulized therapeutic mRNA to the lungs, Nat. Biomed. Eng. 5 (2021) 1059–1068, https://doi.org/10.1038/s41551-021-00786-x.
[96] J. Kim, A. Jozic, Y. Lin, Y. Eygeris, E. Bloom, X. Tan, C. Acosta, K.D. MacDonald, K.D. Welsher, G. Sahay, Engineering lipid nanoparticles for enhanced intracellular delivery of mRNA through inhalation, ACS Nano 16 (2022) 14792–14806, https://doi.org/10.1021/acsnano.2c05647.
[97] M. Ongun, A.G. Lokras, S. Baghel, Z. Shi, S.T. Schmidt, H. Franzyk, T. Rades, F. Sebastiani, A. Thakur, C. Foged, Lipid nanoparticles for local delivery of mRNA to the respiratory tract: effect of PEG-lipid content and administration route, Eur. J. Pharm. Biopharm. 198 (2024), https://doi.org/10.1016/j.ejpb.2024.114266.
[98] H. Miao, K. Huang, Y. Li, R. Li, X. Zhou, J. Shi, Z. Tong, Z. Sun, A. Yu, Optimization of formulation and atomization of lipid nanoparticles for the inhalation of mRNA, Int. J. Pharm. 640 (2023), https://doi.org/10.1016/j.ijpharm.2023.123050.
[99] H. Abbasi, Analyzing Stability and Protein Interaction of RNA Loaded “Onpattro TM” Lipid Nanoparticle, 2023.
[100] F. Sebastiani, M. Yanez Arteta, M. Lerche, L. Porcar, C. Lang, R.A. Bragg, C. S. Elmore, V.R. Krishnamurthy, R.A. Russell, T. Darwish, H. Pichler, S. Waldie, M. Moulin, M. Haertlein, V.T. Forsyth, L. Lindfors, M. Cárdenas, Apolipoprotein E

binding drives structural and compositional rearrangement of mRNA-containing lipid nanoparticles, ACS Nano 15 (2021) 6709–6722, https://doi.org/10.1021/acsnano.0c10064.
[101] Y. Suzuki, H. Ishihara, Structure, activity and uptake mechanism of siRNA-lipid nanoparticles with an asymmetric ionizable lipid, Int. J. Pharm. 510 (2016) 350–358, https://doi.org/10.1016/j.ijpharm.2016.06.124.
[102] K. Fischer, M. Schmidt, Pitfalls and novel applications of particle sizing by dynamic light scattering, Biomaterials 98 (2016) 79–91, https://doi.org/10.1016/j.biomaterials.2016.05.003.
[103] L. Nuhn, S. Gietzen, K. Mohr, K. Fischer, K. Toh, K. Miyata, Y. Matsumoto, K. Kataoka, M. Schmidt, R. Zentel, Aggregation behavior of cationic nanohydrogel particles in human blood serum, Biomacromolecules 15 (2014) 1526–1533, https://doi.org/10.1021/bm500199h.
[104] K. Rausch, A. Reuter, K. Fischer, M. Schmidt, Evaluation of nanoparticle aggregation in human blood serum, Biomacromolecules 11 (2010) 2836–2839, https://doi.org/10.1021/bm100971q.
[105] S.C. Wilson, J.L. Baryza, A.J. Reynolds, K. Bowman, M.E. Keegan, S.M. Standley, N.P. Gardner, P. Parmar, V.O. Agir, S. Yadav, A. Zunic, C. Vargeese, C.C. Lee, S. Rajan, Real time measurement of PEG shedding from lipid nanoparticles in serum via NMR spectroscopy, Mol. Pharm. 12 (2015) 386–392, https://doi.org/10.1021/mp500400k.
[106] Y. Huang, M. Yang, N. Wang, S. Li, Z. Liu, Z. Li, Z. Ji, B. Li, Intracellular delivery of messenger RNA to macrophages with surfactant-derived lipid nanoparticles, Mater Today Adv 16 (2022), https://doi.org/10.1016/j.mtadv.2022.100295.
[107] D. Mehn, F. Caputo, M. Rösslein, L. Calzolai, F. Saint-Antonin, T. Courant, P. Wick, D. Gilliland, Larger or more? Nanoparticle characterisation methods for recognition of dimers, RSC Adv. 7 (2017) 27747–27754, https://doi.org/10.1039/c7ra02432k.
[108] F. Varenne, A. Makky, M. Gaucher-Delmas, F. Violleau, C. Vauthier, Multimodal dispersion of nanoparticles: a comprehensive evaluation of size distribution with 9 size measurement methods, Pharm. Res. 33 (2016) 1220–1234, https://doi.org/10.1007/s11095-016-1867-7.
[109] C.M. Maguire, M. Rösslein, P. Wick, A. Prina-Mello, Characterisation of particles in solution–a perspective on light scattering and comparative technologies, Sci. Technol. Adv. Mater. 19 (2018) 732–745, https://doi.org/10.1080/14686996.2018.1517587.
[110] S. Schmitt, L. Nuhn, M. Barz, H.J. Butt, K. Koynov, Shining Light on Polymeric Drug Nanocarriers with Fluorescence Correlation Spectroscopy, Macromol. Rapid Commun. (2022) 2100892, https://doi.org/10.1002/marc.202100892.
[111] I. Negwer, A. Best, M. Schinnerer, O. Schäfer, L. Capeloa, M. Wagner, M. Schmidt, V. Mailänder, M. Helm, M. Barz, H.J. Butt, K. Koynov, Monitoring drug nanocarriers in human blood by near-infrared fluorescence correlation spectroscopy, Nat. Commun. 9 (2018), https://doi.org/10.1038/s41467-018-07755-0.
[112] H. Zhang, S.C. De Smedt, K. Remaut, Fluorescence correlation spectroscopy to find the critical balance between extracellular association and intracellular dissociation of mRNA complexes, Acta Biomater. 75 (2018) 358–370, https://doi.org/10.1016/j.actbio.2018.05.016.
[113] H. Zhang, K. Rombouts, L. Raes, R. Xiong, S.C. De Smedt, K. Braeckmans, K. Remaut, Fluorescence-based quantification of messenger RNA and plasmid DNA decay kinetics in extracellular biological fluids and cell extracts, Adv. Biosyst. 4 (2020) 2000057, https://doi.org/10.1002/adbi.202000057.
[114] X. Fu, P. Sompol, J.A. Brandon, C.M. Norris, T. Wilkop, L.A. Johnson, C. I. Richards, In vivo single-molecule detection of nanoparticles for multiphoton fluorescence correlation spectroscopy to quantify cerebral blood flow, Nano Lett. 20 (2020) 6135–6141, https://doi.org/10.1021/acs.nanolett.0c02280.
[115] K. Buyens, B. Lucas, K. Raemdonck, K. Braeckmans, J. Vercammen, J. Hendrix, Y. Engelborghs, S.C. De Smedt, N.N. Sanders, A fast and sensitive method for measuring the integrity of siRNA-carrier complexes in full human serum, J. Control. Release 126 (2008) 67–76, https://doi.org/10.1016/j.jconrel.2007.10.024.
[116] K. Remaut, B. Lucas, K. Braeckmans, N. Sanders, S. De Smedt, J. Demeester, Fluorescence correlation spectroscopy to study the degradation of oligonucleotides, both naked and complexed, to cationic carriers, J. Control. Release 132 (2008) e1–e18, https://doi.org/10.1016/j.jconrel.2008.09.048.
[117] G.R. Dakwar, K. Braeckmans, J. Demeester, W. Ceelen, S.C. De Smedt, K. Remaut, Disregarded effect of biological fluids in siRNA delivery: human ascites fluid severely restricts cellular uptake of nanoparticles, ACS Appl. Mater. Interfaces 7 (2015) 23422–24329, https://doi.org/10.1021/acsami.5b08805.
[118] P. Schneider, H. Zhang, L. Simic, Z. Dai, B. Schrörs, Ö. Akilli-Öztürk, J. Lin, F. Durak, J. Schunke, V. Bolduan, B. Bogaert, D. Schwiertz, G. Schäfer, M. Bros, S. Grabbe, J.M. Schattenberg, K. Raemdonck, K. Koynov, M. Diken, L. Kaps, M. Barz, Multicompartment Polyion complex micelles based on triblock Polypept(o)ides mediate efficient siRNA delivery to Cancer-associated fibroblasts for Antistromal therapy of hepatocellular carcinoma, Adv. Mater. (2024), https://doi.org/10.1002/adma.202404784.
[119] T. Sych, J. Schlegel, H.M.G. Barriga, M. Ojansivu, L. Hanke, F. Weber, R. Beklem Bostancioglu, K. Ezzat, H. Stangl, B. Plochberger, J. Laurencikiene, S. El Andaloussi, D. Fürth, M.M. Stevens, E. Sezgin, High-throughput measurement of the content and properties of nano-sized bioparticles with single-particle profiler, Nat. Biotechnol. 42 (2024) 587–590, https://doi.org/10.1038/s41587-023-01825-5.
[120] W. Anderson, D. Kozak, V.A. Coleman, Å.K. Jämting, M. Trau, A comparative study of submicron particle sizing platforms: accuracy, precision and resolution analysis of polydisperse particle size distributions, J. Colloid Interface Sci. 405 (2013) 322–330, https://doi.org/10.1016/j.jcis.2013.02.030.
[121] S. Gioria, F. Caputo, P. Urbán, C.M. Maguire, S. Bremer-Hoffmann, A. Prina-Mello, L. Calzolai, D. Mehn, Are existing standard methods suitable for the evaluation of nanomedicines: Some case studies, Nanomedicine 13 (2018) 539–554, https://doi.org/10.2217/nnm-2017-0338.
[122] M. Berger, M. Degey, J. Leblond Chain, E. Maquoi, B. Evrard, A. Lechanteur, G. Piel, Effect of PEG anchor and serum on lipid nanoparticles: development of a nanoparticles tracking method, Pharmaceutics 15 (2023), https://doi.org/10.3390/pharmaceutics15020597.
[123] V. D'Atri, M. Imiołek, C. Quinn, A. Finny, M. Lauber, S. Fekete, D. Guillarme, Size exclusion chromatography of biopharmaceutical products: from current practices for proteins to emerging trends for viral vectors, nucleic acids and lipid nanoparticles, J. Chromatogr. A 1722 (2024), https://doi.org/10.1016/j.chroma.2024.464862.
[124] X. Jia, Y. Liu, A.M. Wagner, M. Chen, Y. Zhao, K.J. Smith, D. Some, A.M. Abend, J. Pennington, Enabling online determination of the size-dependent RNA content of lipid nanoparticle-based RNA formulations, J. Chromatogr. B Anal. Technol. Biomed. Life Sci. 1186 (2021), https://doi.org/10.1016/j.jchromb.2021.123015.
[125] A. Goyon, S. Tang, S. Fekete, D. Nguyen, K. Hofmann, S. Wang, W. Shatz-Binder, K.I. Fernandez, E.S. Hecht, M. Lauber, K. Zhang, Separation of plasmid DNA topological forms, messenger RNA, and lipid nanoparticle aggregates using an Ultrawide pore size exclusion chromatography column, Anal. Chem. 95 (2023) 15017–15024, https://doi.org/10.1021/acs.analchem.3c02944.
[126] F. Caputo, D. Mehn, J.D. Clogston, M. Rösslein, A. Prina-Mello, S.E. Borgos, S. Gioria, L. Calzolai, Asymmetric-flow field-flow fractionation for measuring particle size, drug loading and (in)stability of nanopharmaceuticals. The joint view of European Union Nanomedicine Characterization Laboratory and National Cancer Institute - Nanotechnology Characterization Laboratory, J. Chromatogr. A 2021 (1635), https://doi.org/10.1016/j.chroma.2020.461767.
[127] F. Caputo, A. Arnould, M. Bacia, W.L. Ling, E. Rustique, I. Texier, A.P. Mello, A. C. Couffin, Measuring particle size distribution by asymmetric flow field flow fractionation: a powerful method for the preclinical characterization of lipid-based nanoparticles, Mol. Pharm. 16 (2019) 756–767, https://doi.org/10.1021/acs.molpharmaceut.8b01033.
[128] R. Mildner, S. Hak, J. Parot, A. Hyldbakk, S.E. Borgos, D. Some, C. Johann, F. Caputo, Improved multidetector asymmetrical-flow field-flow fractionation method for particle sizing and concentration measurements of lipid-based nanocarriers for RNA delivery, Eur. J. Pharm. Biopharm. 163 (2021) 252–265, https://doi.org/10.1016/j.ejpb.2021.03.004.
[129] M.A. Graewert, C. Wilhelmy, T. Bacic, J. Schumacher, C. Blanchet, F. Meier, R. Drexel, R. Welz, B. Kolb, K. Bartels, T. Nawroth, T. Klein, D. Svergun, P. Langguth, H. Haas, Quantitative size-resolved characterization of mRNA nanoparticles by in-line coupling of asymmetrical-flow field-flow fractionation with small angle X-ray scattering, Sci. Rep. 13 (2023), https://doi.org/10.1038/s41598-023-42274-z.
[130] R. Holland, K. Lam, S. Jeng, K. McClintock, L. Palmer, P. Schreiner, M. Wood, W. Zhao, J. Heyes, Silicon ether Ionizable lipids enable potent mRNA lipid nanoparticles with rapid tissue clearance, ACS Nano 18 (2024) 10374–10387, https://doi.org/10.1021/acsnano.3c09028.
[131] Y. Xu, M. Ou, E. Keough, J. Roberts, K. Koeplinger, M. Lyman, S. Fauty, E. Carlini, M. Stern, R. Zhang, S. Yeh, E. Mahan, Y. Wang, D. Slaughter, M. Gindy, C. Raab, C. Thompson, J. Hochman, Quantitation of physiological and biochemical barriers to siRNA liver delivery via lipid nanoparticle platform, Mol. Pharm. 11 (2014) 1424–1434, https://doi.org/10.1021/mp400584h.
[132] W.L. van Os, L. Wielaert, C. Alter, D. Davidović, R. Šachl, T. Kock, U.U. González, G. Arias-Alpizar, F.L. Vigario, R.A. Knol, R. Kuster, S. Romeijn, N.L. Mora, P. Detampel, M. Hof, J. Huwyler, A. Kros, Lipid conjugate dissociation analysis improves the in vivo understanding of lipid-based nanomedicine, J. Control. Release 371 (2024) 85–100, https://doi.org/10.1016/j.jconrel.2024.05.034.
[133] R.J. Mow, A. Srinivasan, E. Bolay, D. Merlin, C. Yang, Fluorescent labeling and imaging of IL-22 mRNA-loaded lipid nanoparticles, Bio-Protoc. 14 (2024), https://doi.org/10.21769/BioProtoc.4994.
[134] R. Ma, Y. Li, Y. Wei, J. Zhou, J. Ma, M. Zhang, J. Tu, J. Jiang, S. Xie, W. Tan, X. Liu, The dynamic process of mRNA delivery by lipid nanoparticles in vivo, Nano Today 57 (2024), https://doi.org/10.1016/j.nantod.2024.102325.
[135] C.A. Alabi, K.T. Love, G. Sahay, T. Stutzman, W.T. Young, R. Langer, D. G. Anderson, FRET-labeled siRna probes for tracking assembly and disassembly of sirna nanocomplexes, ACS Nano 6 (2012) 6133–6141, https://doi.org/10.1021/nn3013838.
[136] C.A. Alabi, K.T. Love, G. Sahay, H. Yin, K.M. Luly, R. Langer, D.G. Anderson, Multiparametric approach for the evaluation of lipid nanoparticles for siRNA delivery, Proc. Natl. Acad. Sci. USA 110 (2013) 12881–12886, https://doi.org/10.1073/pnas.1306529110.
[137] R. van der Meel, S. Chen, J. Zaifman, J.A. Kulkarni, X.R.S. Zhang, Y.K. Tam, M. B. Bally, R.M. Schiffelers, M.A. Ciufolini, P.R. Cullis, Y.Y.C. Tam, Modular lipid nanoparticle platform technology for siRNA and lipophilic prodrug delivery, Small 17 (2021), https://doi.org/10.1002/smll.202103025.
[138] K.E. Lindsay, S.M. Bhosle, C. Zurla, J. Beyersdorf, K.A. Rogers, D. Vanover, P. Xiao, M. Araínga, L.M. Shirreff, B. Pitard, P. Baumhof, F. Villinger, P. J. Santangelo, Visualization of early events in mRNA vaccine delivery in non-human primates via PET–CT and near-infrared imaging, Nat Biomed Eng 3 (2019) 371–380, https://doi.org/10.1038/s41551-019-0378-3.
[139] M. Buckley, M. Araínga, L. Maiorino, I.S. Pires, B.J. Kim, K. Kaczmarek Michaels, J. Dye, K. Qureshi, Y. Zhang, H. Mak, J.M. Steichen, W.R. Schief, F. Villinger, D. J. Irvine, Visualizing lipid nanoparticle trafficking for mRNA vaccine delivery in non-human primates, 2025, https://doi.org/10.1101/2024.06.21.600088.

[140] C. Chen, C. Chen, Y. Li, R. Gu, X. Yan, Characterization of lipid-based nanomedicines at the single-particle level, Fundamental Research 3 (2023) 488–504, https://doi.org/10.1016/j.fmre.2022.09.011.
[141] M.Y. Arteta, T. Kjellman, S. Bartesaghi, S. Wallin, X. Wu, A.J. Kvist, A. Dabkowska, N. Székely, A. Radulescu, J. Bergenholtz, L. Lindfors, Successful reprogramming of cellular protein production through mRNA delivered by functionalized lipid nanoparticles, Proc. Natl. Acad. Sci. USA 115 (2018) E3351–E3360, https://doi.org/10.1073/pnas.1720542115.
[142] R. Crawford, B. Dogdas, E. Keough, R.M. Haas, W. Wepukhulu, S. Krotzer, P. A. Burke, L. Sepp-Lorenzino, A. Bagchi, B.J. Howell, Analysis of lipid nanoparticles by Cryo-EM for characterizing siRNA delivery vehicles, Int. J. Pharm. 403 (2011) 237–244, https://doi.org/10.1016/j.ijpharm.2010.10.025.
[143] T. Tasdizen, E. Jurrus, R.T. Whitaker, Non-Uniform Illumination Correction In Transmission Electron Microscopy, 2025.
[144] V. Francia, Y. Zhang, M.H. Yan Cheng, R.M. Schiffelers, D. Witzigmann, P. R. Cullis, A magnetic separation method for isolating and characterizing the biomolecular corona of lipid nanoparticles, Proc. Natl. Acad. Sci. USA 121 (2024), https://doi.org/10.1073/pnas.2307803120.
[145] M. Almgren, K. Edwards, G. Ran Karlsson, Cryo Transmission electron Microscopy of Liposomes and Related Structures. www.elsevier.nl/locate/colsurfa, 2000.
[146] G.L. Hura, A.L. Menon, M. Hammel, R.P. Rambo, F.L. Poole, S.E. Tsutakawa, F. E. Jenney, S. Classen, K.A. Frankel, R.C. Hopkins, S.J. Yang, J.W. Scott, B. D. Dillard, M.W.W. Adams, J.A. Tainer, Robust, high-throughput solution structural analyses by small angle X-ray scattering (SAXS), Nat. Methods 6 (2009) 606–612, https://doi.org/10.1038/nmeth.1353.
[147] C. Wilhelmy, I.S. Keil, L. Uebbing, M.A. Schroer, D. Franke, T. Nawroth, M. Barz, U. Sahin, H. Haas, M. Diken, P. Langguth, Polysarcosine-functionalized mRNA lipid nanoparticles tailored for immunotherapy, Pharmaceutics 15 (2023), https://doi.org/10.3390/pharmaceutics15082068.
[148] A. Gallud, M.J. Munson, K. Liu, A. Idström, H.M.G. Barriga, S.R. Tabaei, N. Aliakbarinodehi, M. Ojansivu, Q. Lubart, J.J. Doutch, M.N. Holme, L. Evenäs, L. Lindfors, M.M. Stevens, A. Collén, A. Sabirsh, F. Höök, A.E.K. Esbjörner, Time evolution of PEG-shedding and serum protein coronation determines the cell uptake kinetics and delivery of lipid nanoparticle formulated mRNA, 2025, https://doi.org/10.1101/2021.08.20.457104.
[149] L. Caselli, L. Conti, I. De Santis, D. Berti, Small-angle X-ray and neutron scattering applied to lipid-based nanoparticles: recent advancements across different length scales, Adv. Colloid Interf. Sci. 327 (2024), https://doi.org/10.1016/j.cis.2024.103156.
[150] M. Li, S. Li, Y. Huang, H. Chen, S. Zhang, Z. Zhang, W. Wu, X. Zeng, B. Zhou, B. Li, Secreted expression of mRNA-encoded truncated ACE2 variants for SARS-CoV-2 via lipid-like Nanoassemblies, Adv. Mater. 33 (2021), https://doi.org/10.1002/adma.202101707.
[151] Y. Huang, M. Yang, N. Wang, S. Li, Z. Liu, Z. Li, Z. Ji, B. Li, Intracellular delivery of messenger RNA to macrophages with surfactant-derived lipid nanoparticles, Mater Today Adv 16 (2022), https://doi.org/10.1016/j.mtadv.2022.100295.
[152] C. Malburet, L. Leclercq, J.F. Cotte, J. Thiebaud, E. Bazin, M. Garinot, H. Cottet, Taylor dispersion analysis to support lipid-nanoparticle formulations for mRNA vaccines, Gene Ther. 30 (2023) 421–428, https://doi.org/10.1038/s41434-022-00370-1.
[153] X. Zhang, V. Goel, G.J. Robbie, Pharmacokinetics of Patisiran, the first approved RNA interference therapy in patients with hereditary transthyretin-mediated amyloidosis, J. Clin. Pharmacol. 60 (2020) 573–585, https://doi.org/10.1002/jcph.1553.
[154] D. Shi, D. Beasock, A. Fessler, J. Szebeni, J.Y. Ljubimova, K.A. Afonin, M. A. Dobrovolskaia, To PEGylate or not to PEGylate: immunological properties of nanomedicine's most popular component, polyethylene glycol and its alternatives, Adv. Drug Deliv. Rev. 180 (2022), https://doi.org/10.1016/j.addr.2021.114079.
[155] L. Shen, Z. Li, A. Ma, C. Cruz-Teran, A. Talkington, S.T. Shipley, S.K. Lai, Free PEG suppresses anaphylaxis to PEGylated nanomedicine in swine, ACS Nano 18 (2023), https://doi.org/10.1021/ACSNANO.3C11165/ASSET/IMAGES/LARGE/NN3C11165_0005.JPEG.
[156] M. Estapé Senti, C.A. de Jongh, K. Dijkxhoorn, J.J.F. Verhoef, J. Szebeni, G. Storm, C.E. Hack, R.M. Schiffelers, M.H. Fens, P. Boross, Anti-PEG antibodies compromise the integrity of PEGylated lipid-based nanoparticles via complement, J. Control. Release 341 (2022) 475–486, https://doi.org/10.1016/j.jconrel.2021.11.042.
[157] G.T. Kozma, T. Shimizu, T. Ishida, J. Szebeni, Anti-PEG antibodies: properties, formation, testing and role in adverse immune reactions to PEGylated nano-biopharmaceuticals, Adv. Drug Deliv. Rev. 154–155 (2020) 163–175, https://doi.org/10.1016/j.addr.2020.07.024.
[158] Q. Yang, S.K. Lai, Anti-PEG immunity: emergence, characteristics, and unaddressed questions, Nanomedicine and Nanobiotechnology 7 (2015) 655–677, https://doi.org/10.1002/WNAN.1339.
[159] Y. Ju, J.M. Carreño, V. Simon, K. Dawson, F. Krammer, S.J. Kent, Impact of anti-PEG antibodies induced by SARS-CoV-2 mRNA vaccines, Nat. Rev. Immunol. 23 (2023) 135–136, https://doi.org/10.1038/s41577-022-00825-x.
[160] Y. Ju, W.S. Lee, E.H. Pilkington, H.G. Kelly, S. Li, K.J. Selva, K.M. Wragg, K. Subbarao, T.H.O. Nguyen, L.C. Rowntree, L.F. Allen, K. Bond, D.A. Williamson, N.P. Truong, M. Plebanski, K. Kedzierska, S. Mahanty, A.W. Chung, F. Caruso, A. K. Wheatley, J.A. Juno, S.J. Kent, Anti-PEG antibodies boosted in humans by SARS-CoV-2 lipid nanoparticle mRNA vaccine, ACS Nano 16 (2022) 11769–11780, https://doi.org/10.1021/acsnano.2c04543.
[161] A.R. Irizarry Rovira, B.M. Bennet, B. Bolon, A. Braendli-Baiocco, S. Chandra, R. Fleurance, R. Garman, D. Hutto, J. Lane, A. Romeike, A. Sargeant, B. Zimmerman, Scientific and regulatory policy committee points to consider: histopathologic evaluation in safety assessment studies for PEGylated pharmaceutical products, Toxicol. Pathol. 46 (2018) 616–635, https://doi.org/10.1177/0192623318791801.
[162] M. Barz, R. Luxenhofer, R. Zentel, M.J. Vicent, Overcoming the PEG-addiction: well-defined alternatives to PEG, from structure-property relationships to better defined therapeutics, Polym. Chem. 2 (2011) 1900–1918, https://doi.org/10.1039/c0py00406e.
[163] K. Knop, R. Hoogenboom, D. Fischer, U.S. Schubert, Poly(ethylene glycol) in drug delivery: pros and cons as well as potential alternatives, Angew. Chem. Int. Ed. 49 (2010) 6288–6308, https://doi.org/10.1002/anie.200902672.
[164] H. Bayraktutan, R.J. Kopiasz, A. Elsherbeny, M. Martinez Espuga, N. Gumus, U. C. Oz, K. Polra, P.F. McKay, R.J. Shattock, P. Ordóñez-Morán, A. Mata, C. Alexander, P. Gurnani, Polysarcosine functionalised cationic polyesters efficiently deliver self-amplifying mRNA, Polym. Chem. 15 (2024) 1862–1876, https://doi.org/10.1039/d4py00064a.
[165] M.F. Kabil, H.M.E.S. Azzazy, M. Nasr, Recent progress on polySarcosine as an alternative to PEGylation: synthesis and biomedical applications, Int. J. Pharm. 653 (2024), https://doi.org/10.1016/j.ijpharm.2024.123871.
[166] A. Birke, J. Ling, M. Barz, Polysarcosine-containing copolymers: synthesis, characterization, self-assembly, and applications, Prog. Polym. Sci. 81 (2018) 163–208.
[167] G. Settanni, T. Schäfer, C. Muhl, M. Barz, F. Schmid, Poly-sarcosine and poly (ethylene-glycol) interactions with proteins investigated using molecular dynamics simulations, Comput Struct, Biotechnol. J. 16 (2018) 543–550, https://doi.org/10.1016/j.csbj.2018.10.012.
[168] T.A. Bauer, L. Simić, J.F.R. Van Guyse, A. Duro-Castaño, V.J. Nebot, M. Barz, Polypept(o)ides – origins, synthesis, applications and future directions, Prog. Polym. Sci. (2024) 101889, https://doi.org/10.1016/j.progpolymsci.2024.101889.
[169] M. Hu, K. Taguchi, K. Matsumoto, E. Kobatake, Y. Ito, M. Ueda, Polysarcosine-coated liposomes attenuating immune response induction and prolonging blood circulation, J. Colloid Interface Sci. 651 (2023) 273–283, https://doi.org/10.1016/j.jcis.2023.07.149.
[170] D. Bi, D.M. Unthan, L. Hu, J. Bussmann, K. Remaut, M. Barz, H. Zhang, Polysarcosine-based lipid formulations for intracranial delivery of mRNA, J. Control. Release 356 (2023) 1–13, https://doi.org/10.1016/j.jconrel.2023.02.021.
[171] D.D. Kang, X. Hou, L. Wang, Y. Xue, H. Li, Y. Zhong, S. Wang, B. Deng, D. W. McComb, Y. Dong, Engineering LNPs with polysarcosine lipids for mRNA delivery, Bioact Mater 37 (2024) 86–93, https://doi.org/10.1016/j.bioactmat.2024.03.017.
[172] R. Tan, G. Huang, C. Wei, Z. He, T. Zhao, Y. Shi, Z. Liu, Y. Chen, Influence of structural variations in polysarcosine functionalized lipids on lipid nanoparticle-mediated mRNA delivery, J. Polym. Sci. (2024), https://doi.org/10.1002/pol.20240154.
[173] G. Hayes, B. Dias-Barbieri, G. Yilmaz, R.J. Shattock, C.R. Becer, Poly(2-oxazoline)/saRNA Polyplexes for targeted and nonviral gene delivery, Biomacromolecules 24 (2023) 5142–5151, https://doi.org/10.1021/acs.biomac.3c00683.
[174] A. Zahoranová, R. Luxenhofer, Poly(2-oxazoline)- and poly(2-oxazine)-based self-assemblies, Polyplexes, and drug Nanoformulations—an update, Adv. Healthc. Mater. 10 (2021), https://doi.org/10.1002/adhm.202001382.
[175] D.N. Yamaleyeva, N. Makita, D. Hwang, M.J. Haney, R. Jordan, A.V. Kabanov, Poly(2-oxazoline)-based Polyplexes as a PEG-free plasmid DNA delivery platform, Macromol. Biosci. 23 (2023), https://doi.org/10.1002/mabi.202300177.
[176] M.N. Leiske, M. Lai, T. Amarasena, T.P. Davis, K.J. Thurecht, S.J. Kent, K. Kempe, Interactions of core cross-linked poly(2-oxazoline) and poly(2-oxazine) micelles with immune cells in human blood, Biomaterials 274 (2021), https://doi.org/10.1016/j.biomaterials.2021.120843.
[177] B. Li, F. Chu, Q. Lu, Y. Wang, L.A. Lane, Alternating stealth polymer coatings between administrations minimizes toxic and antibody immune responses towards nanomedicine treatment regimens, Acta Biomater. 121 (2021) 527–540, https://doi.org/10.1016/j.actbio.2020.11.047.
[178] M.C. Woodle, C.M. Engbers, S. Zalipsky, New Amphipatic Polymer-Lipid Conjugates Forming Long-Circulating Reticuloendothelial System-Evading Liposomes, 1994.
[179] J.F.R. Van Guyse, S. Abbasi, K. Toh, Z. Nagorna, J. Li, A. Dirisala, S. Quader, S. Uchida, K. Kataoka, Facile generation of Heterotelechelic poly(2-Oxazoline)s towards accelerated exploration of poly(2-Oxazoline)-based nanomedicine, Angew. Chem. Int. Ed. 63 (2024), https://doi.org/10.1002/anie.202404972.
[180] T.X. Viegas, M.D. Bentley, J.M. Harris, Z. Fang, K. Yoon, B. Dizman, R. Weimer, A. Mero, G. Pasut, F.M. Veronese, Polyoxazoline: chemistry, properties, and applications in drug delivery, Bioconjug. Chem. 22 (2011) 976–986, https://doi.org/10.1021/bc200049d.
[181] M. Bauer, C. Lautenschlaeger, K. Kempe, L. Tauhardt, U.S. Schubert, D. Fischer, Poly(2-ethyl-2-oxazoline) as alternative for the stealth polymer poly(ethylene glycol): comparison of in vitro cytotoxicity and Hemocompatibility, Macromol. Biosci. 12 (2012) 986–998, https://doi.org/10.1002/mabi.201200017.
[182] M. Berger, F. Toussaint, S. Ben Djemaa, J. Laloy, H. Pendeville, B. Evrard, C. Jerôme, A. Lechanteur, D. Mottet, A. Debuigne, G. Piel, Poly(vinyl pyrrolidone) derivatives as PEG alternatives for stealth, non-toxic and less immunogenic siRNA-containing lipoplex delivery, J. Control. Release 361 (2023) 87–101, https://doi.org/10.1016/j.jconrel.2023.07.031.
[183] M. Berger, F. Toussaint, S. Ben Djemaa, E. Maquoi, H. Pendeville, B. Evrard, C. Jerôme, J. Leblond Chain, A. Lechanteur, D. Mottet, A. Debuigne, G. Piel, Poly

(N-methyl-N-vinylacetamide): a Strong alternative to PEG for lipid-based Nanocarriers delivering siRNA, Adv. Healthc. Mater. 13 (2024), https://doi.org/10.1002/adhm.202302712.
[184] J.B. Schlenoff, Zwitteration: coating surfaces with zwitterionic functionality to reduce nonspecific adsorption, Langmuir 30 (2014) 9625–9636, https://doi.org/10.1021/la500057j.
[185] M.A. Jackson, T.A. Werfel, E.J. Curvino, F. Yu, T.E. Kavanaugh, S.M. Sarett, M. D. Dockery, K.V. Kilchrist, A.N. Jackson, T.D. Giorgio, C.L. Duvall, Zwitterionic Nanocarrier surface chemistry improves siRNA tumor delivery and silencing activity relative to polyethylene glycol, ACS Nano 11 (2017) 5680–5696, https://doi.org/10.1021/acsnano.7b01110.
[186] W. Lin, R. Goldberg, J. Klein, Poly-phosphocholination of liposomes leads to highly-extended retention time in mice joints, J. Mater. Chem. B 10 (2022) 2820–2827, https://doi.org/10.1039/d1tb02346b.
[187] P.O. Khunsuk, C. Pongma, T. Palaga, V.P. Hoven, Zwitterionic polymer-decorated lipid nanoparticles for mRNA delivery in mammalian cells, Biomacromolecules 24 (2023) 5654–5665, https://doi.org/10.1021/acs.biomac.3c00649.
[188] S. Acosta-Gutiérrez, D. Matias, M. Avila-Olias, V.M. Gouveia, E. Scarpa, J. Forth, C. Contini, A. Duro-Castano, L. Rizzello, G. Battaglia, A multiscale study of Phosphorylcholine driven cellular phenotypic targeting, ACS Cent Sci 8 (2022) 891–904, https://doi.org/10.1021/acscentsci.2c00146.
[189] M. Massignani, C. Lopresti, A. Blanazs, J. Madsen, S.P. Armes, A.L. Lewis, G. Battaglia, Controlling cellular uptake by surface chemistry, size, and surface topology at the nanoscale, Small 5 (2009) 2424–2432, https://doi.org/10.1002/smll.200900578.
[190] W. Yang, S. Liu, T. Bai, A.J. Keefe, L. Zhang, J.R. Ella-Menye, Y. Li, S. Jiang, Poly (carboxybetaine) nanomaterials enable long circulation and prevent polymer-specific antibody production, Nano Today 9 (2014) 10–16, https://doi.org/10.1016/j.nantod.2014.02.004.
[191] Y. Li, R. Liu, Y. Shi, Z. Zhang, X. Zhang, Zwitterionic poly(carboxybetaine)-based cationic liposomes for effective delivery of small interfering RNA therapeutics without accelerated blood clearance phenomenon, Theranostics 5 (2015) 583–596, https://doi.org/10.7150/thno.11234.
[192] Y.J. Sung, H. Guo, A. Ghasemizadeh, X. Shen, W. Chintrakulchai, M. Kobayashi, M. Toyoda, K. Ogi, J. Michinishi, T. Ohtake, M. Matsui, Y. Honda, T. Nomoto, H. Takemoto, Y. Miura, N. Nishiyama, Cancerous pH-responsive polycarboxybetaine-coated lipid nanoparticle for smart delivery of siRNA against subcutaneous tumor model in mice, Cancer Sci. 113 (2022) 4339–4349, https://doi.org/10.1111/cas.15554.
[193] K. Homma, Y. Miura, M. Kobayashi, W. Chintrakulchai, M. Toyoda, K. Ogi, J. Michinishi, T. Ohtake, Y. Honda, T. Nomoto, H. Takemoto, N. Nishiyama, Fine tuning of the net charge alternation of polyzwitterion surfaced lipid nanoparticles to enhance cellular uptake and membrane fusion potential, Sci. Technol. Adv. Mater. 25 (2024), https://doi.org/10.1080/14686996.2024.2338785.